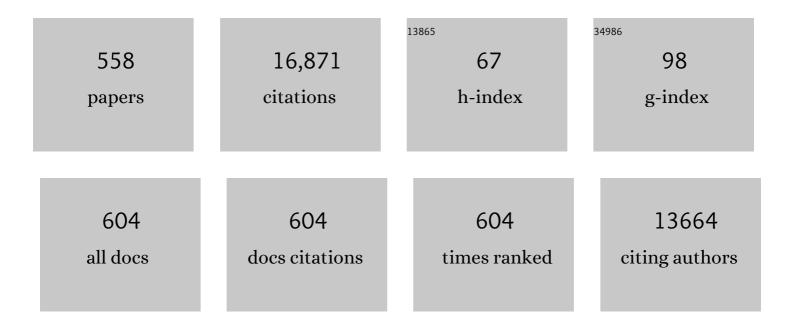
Kohei Uosaki

List of Publications by Year in descending order

Source: https://exaly.com/author-pdf/1862115/publications.pdf Version: 2024-02-01



#	Article	IF	CITATIONS
1	Preparation of Polycrystalline TiO2Photocatalysts Impregnated with Various Transition Metal Ions:Â Characterization and Photocatalytic Activity for the Degradation of 4-Nitrophenol. Journal of Physical Chemistry B, 2002, 106, 637-645.	2.6	460
2	Electrochemical characteristics of a gold electrode modified with a self-assembled monolayer of ferrocenylalkanethiols. Langmuir, 1991, 7, 1510-1514.	3.5	318
3	Very Efficient Visible-Light-Induced Uphill Electron Transfer at a Self-Assembled Monolayer with a Porphyrinâ^Ferroceneâ^Thiol Linked Molecule. Journal of the American Chemical Society, 1997, 119, 8367-8368.	13.7	282
4	Boron Nitride Nanosheet on Gold as an Electrocatalyst for Oxygen Reduction Reaction: Theoretical Suggestion and Experimental Proof. Journal of the American Chemical Society, 2014, 136, 6542-6545.	13.7	231
5	Quantitative analysis of defective sites in titanium(IV) oxide photocatalyst powders. Physical Chemistry Chemical Physics, 2003, 5, 778-783.	2.8	217
6	Fabrication and Characterization of CdS-Nanoparticle Mono- and Multilayers on a Self-Assembled Monolayer of Alkanedithiols on Gold. Journal of Physical Chemistry B, 1998, 102, 1571-1577.	2.6	194
7	Layered Perovskite Oxide: A Reversible Air Electrode for Oxygen Evolution/Reduction in Rechargeable Metal-Air Batteries. Journal of the American Chemical Society, 2013, 135, 11125-11130.	13.7	194
8	Photocatalytic activity of transition-metal-loaded titanium(IV) oxide powders suspended in aqueous solutions: Correlation with electron–hole recombination kinetics. Physical Chemistry Chemical Physics, 2001, 3, 267-273.	2.8	192
9	In situ and dynamic monitoring of the self-assembling and redox processes of a ferrocenylundecanethiol monolayer by electrochemical quartz crystal microbalance. Langmuir, 1992, 8, 1385-1387.	3.5	180
10	In Situ Scanning Tunneling Microscopy Observation of the Self-Assembly Process of Alkanethiols on Gold(111) in Solution. Langmuir, 1998, 14, 855-861.	3.5	174
11	Sum frequency generation (SFG) study of the pH-dependent water structure on a fused quartz surface modified by an octadecyltrichlorosilane (OTS) monolayer. Physical Chemistry Chemical Physics, 2001, 3, 3463-3469.	2.8	171
12	Effect of Temperature on Structure of the Self-Assembled Monolayer of Decanethiol on Au(111) Surface. Langmuir, 2000, 16, 5523-5525.	3.5	146
13	Single Molecule Dynamics at a Mechanically Controllable Break Junction in Solution at Room Temperature. Journal of the American Chemical Society, 2013, 135, 1009-1014.	13.7	138
14	Electrochemical Layer-by-Layer Growth of Palladium on an Au(111) Electrode Surface:  Evidence for Important Role of Adsorbed Pd Complex. Journal of Physical Chemistry B, 1998, 102, 4366-4373.	2.6	132
15	Redox-Induced Orientation Change of a Self-Assembled Monolayer of 11-Ferrocenyl-1-undecanethiol on a Gold Electrode Studied by in Situ FT-IRRAS. Langmuir, 1997, 13, 3157-3161.	3.5	130
16	In Situ, Real Time Monitoring of the Self-Assembly Process of Decanethiol on Au(111) in Liquid Phase. A Scanning Tunneling Microscopy Investigation. Langmuir, 1997, 13, 5218-5221.	3.5	126
17	Role of Cerium Oxide in the Enhancement of Activity for the Oxygen Reduction Reaction at Pt–CeO _{<i>x</i>} Nanocomposite Electrocatalyst - An in Situ Electrochemical X-ray Absorption Fine Structure Study. Journal of Physical Chemistry C, 2012, 116, 10098-10102.	3.1	121
18	Electrochemical Epitaxial Growth of a Pt(111) Phase on an Au(111) Electrode. Journal of Physical Chemistry B, 1997, 101, 7566-7572.	2.6	118

#	Article	IF	CITATIONS
19	Electrocatalytic reactivity for oxygen reduction at epitaxially grown Pd thin layers of various thickness on Au(111) and Au(100). Electrochimica Acta, 2000, 45, 3305-3309.	5.2	116
20	Functionalization of Monolayer h-BN by a Metal Support for the Oxygen Reduction Reaction. Journal of Physical Chemistry C, 2013, 117, 21359-21370.	3.1	109
21	Electrochemical and electrogenerated chemiluminescence properties of tris(2,2′-bipyridine)ruthenium(II)-tridecanethiol derivative on ITO and gold electrodes. Journal of Electroanalytical Chemistry, 1995, 384, 57-66.	3.8	107
22	Femtosecond Diffuse Reflectance Spectroscopy of Aqueous Titanium(IV) Oxide Suspension: Correlation of Electron-Hole Recombination Kinetics with Photocatalytic Activity. Chemistry Letters, 1998, 27, 579-580.	1.3	107
23	Electrochemical properties of the 2-mercaptohydroquinone monolayer on a gold electrode. Effect of solution pH, adsorption time and concentration of the modifying solution. Journal of Electroanalytical Chemistry, 1996, 409, 145-154.	3.8	105
24	Interfacial Water Structure at As-Prepared and UV-Induced Hydrophilic TiO2Surfaces Studied by Sum Frequency Generation Spectroscopy and Quartz Crystal Microbalance. Journal of Physical Chemistry B, 2004, 108, 19086-19088.	2.6	104
25	Structure of Au(111) and Au(100) Single-Crystal Electrode Surfaces at Various Potentials in Sulfuric Acid Solution Determined by In Situ Surface X-ray Scattering. Journal of Physical Chemistry C, 2007, 111, 13197-13204.	3.1	102
26	Electrochemistry of cytochrome c. Comparison of the electron transfer at a surface-modified gold electrode with that to cytochrome oxidase. Journal of the American Chemical Society, 1979, 101, 7113-7114.	13.7	100
27	The Rate of the Photoelectrochemical Generation of Hydrogen at pâ€Type Semiconductors. Journal of the Electrochemical Society, 1977, 124, 1348-1355.	2.9	98
28	Crystal Face Dependent Chemical Effects in Surface-Enhanced Raman Scattering at Atomically Defined Gold Facets. Nano Letters, 2011, 11, 1716-1722.	9.1	98
29	Structural Changes in Poly(2-methoxyethyl acrylate) Thin Films Induced by Absorption of Bisphenol A. An Infrared and Sum Frequency Generation (SFG) Study. Macromolecules, 2003, 36, 5694-5703.	4.8	96
30	Formation of Two-Dimensional Crystals of Alkanes on the Au(111) Surface in Neat Liquid. Journal of the American Chemical Society, 1999, 121, 4090-4091.	13.7	95
31	Theoretical predictions for hexagonal BN based nanomaterials as electrocatalysts for the oxygen reduction reaction. Physical Chemistry Chemical Physics, 2013, 15, 2809.	2.8	95
32	Insulative Microfiber 3D Matrix as a Host Material Minimizing Volume Change of the Anode of Li Metal Batteries. ACS Energy Letters, 2017, 2, 924-929.	17.4	95
33	Dynamic changes in charge-transfer resistance at Li metal/Li7La3Zr2O12 interfaces during electrochemical Li dissolution/deposition cycles. Journal of Power Sources, 2018, 376, 147-151.	7.8	95
34	Thickness dependent electrochemical reactivity of epitaxially electrodeposited palladium thin layers on Au(111) and Au(100) surfaces. Journal of Electroanalytical Chemistry, 2001, 500, 435-445.	3.8	94
35	Electrochemically Controlled Layer-by-Layer Deposition of Metal-Cluster Molecular Multilayers on Gold. Angewandte Chemie - International Edition, 2003, 42, 2912-2915.	13.8	94
36	Basic knowledge in battery research bridging the gap between academia and industry. Materials Horizons, 2020, 7, 1937-1954.	12.2	94

#	Article	IF	CITATIONS
37	Local conformation of poly(methyl methacrylate) at nitrogen and water interfaces. Polymer Chemistry, 2010, 1, 303-311.	3.9	93
38	Dynamic Ellipsometry of a Self-Assembled Monolayer of a Ferrocenylalkanethiol during Oxidation-Reduction Cycles. Langmuir, 1994, 10, 3658-3662.	3.5	92
39	Raman scattering of aryl isocyanide monolayers on atomically flat Au(1 1 1) single crystal surfaces enhanced by gap-mode plasmon excitation. Chemical Physics Letters, 2008, 460, 205-208.	2.6	91
40	<i>In situ</i> x-ray photoelectron spectroscopy for electrochemical reactions in ordinary solvents. Applied Physics Letters, 2013, 103, .	3.3	89
41	Pseudomorphic growth of Pd monolayer on Au(111) electrode surface. Surface Science, 2000, 461, 213-218.	1.9	88
42	Potential-dependent structure of the interfacial water on the gold electrode. Surface Science, 2004, 573, 11-16.	1.9	88
43	Electrochemical quartz crystal microbalance studies of self-assembled monolayers of 11-ferrocenyl-1-undecanethiol: Structure-dependent ion-pairing and solvent uptake. Journal of Electroanalytical Chemistry, 1994, 372, 117-124.	3.8	84
44	Role of Interfacial Water in Protein Adsorption onto Polymer Brushes as Studied by SFG Spectroscopy and QCM. Journal of Physical Chemistry C, 2015, 119, 17193-17201.	3.1	84
45	Preparation of a Highly Ordered Au (111) Phase on a Polycrystalline Gold Substrate by Vacuum Deposition and Its Characterization by XRD, GISXRD, STM/AFM, and Electrochemical Measurements. The Journal of Physical Chemistry, 1995, 99, 14117-14122.	2.9	83
46	Adsorption behavior of functionalized ferrocenylalkane thiols and disulfide onto Au and ITO and electrochemical properties of modified electrodes: Effects of acyl and alkyl groups attached to the ferrocene ring. Journal of Electroanalytical Chemistry, 1995, 381, 203-209.	3.8	80
47	Surface Molecular Structures of Langmuirâ d'Blodgett Films of Stearic Acid on Solid Substrates Studied by Sum Frequency Generation Spectroscopy. Langmuir, 2003, 19, 2238-2242.	3.5	80
48	Effects of Atomic Geometry and Electronic Structure of Platinum Surfaces on Molecular Adsorbates Studied by Gap-Mode SERS. Journal of the American Chemical Society, 2014, 136, 10299-10307.	13.7	80
49	Electrode Potential Effect on the Surface pKa of a Self-Assembled 15-Mercaptohexadecanoic Acid Monolayer on a Gold/Quartz Crystal Microbalance Electrode. Langmuir, 2000, 16, 7101-7105.	3.5	78
50	327 - The electrochemistry of cytochrome c. investigation of the mechanism of the 4,4′-bipyridyl surface modified gold electrode. Bioelectrochemistry, 1980, 7, 527-537.	1.0	76
51	Anisotropic Dissolution of an Au(111) Electrode in Perchloric Acid Solution Containing Chloride Anion Investigated by in Situ STMThe Important Role of Adsorbed Chloride Anion. Langmuir, 1999, 15, 807-812.	3.5	75
52	Activity of oxygen reduction reaction on small amount of amorphous CeO promoted Pt cathode for fuel cell application. Electrochimica Acta, 2011, 56, 3874-3883.	5.2	75
53	In Situ, Real-Time Monitoring of the Reductive Desorption Process of Self-Assembled Monolayers of Hexanethiol on Au(111) Surfaces in Acidic and Alkaline Aqueous Solutions by Scanning Tunneling Microscopy. Langmuir, 2001, 17, 8224-8228.	3.5	74
54	Preparation of Cocrystals of 2-Amino-3-nitropyridine with Benzenesulfonic Acids for Second-Order Nonlinear Optical Materials. Crystal Growth and Design, 2004, 4, 807-811.	3.0	74

#	Article	IF	CITATIONS
55	Control of the Charge-Transfer Rate at a Gold Electrode Modified with a Self-Assembled Monolayer Containing Ferrocene and Azobenzene by Electro- and Photochemical Structural Conversion of Cis and Trans Forms of the Azobenzene Moiety. Langmuir, 2001, 17, 6317-6324.	3.5	73
56	Formation of Nanopatterns of a Self-Assembled Monolayer (SAM) within a SAM of Different Molecules Using a Current Sensing Atomic Force Microscope. Nano Letters, 2002, 2, 137-140.	9.1	73
57	Evolving affinity between Coulombic reversibility and hysteretic phase transformations in nano-structured silicon-based lithium-ion batteries. Nature Communications, 2018, 9, 479.	12.8	73
58	Electrocatalytic reduction of oxygen to water at Au nanoclusters vacuum-evaporated on boron-doped diamond in acidic solution. Electrochemistry Communications, 2004, 6, 773-779.	4.7	72
59	Plasmonic Enhancement of Raman Scattering on Non-SERS-Active Platinum Substrates. Journal of Physical Chemistry C, 2009, 113, 11816-11821.	3.1	72
60	Highly Efficient Electrochemical Hydrogen Evolution Reaction at Insulating Boron Nitride Nanosheet on Inert Gold Substrate. Scientific Reports, 2016, 6, 32217.	3.3	72
61	First observation of electroluminescence at the p-type semiconductor/electrolyte interface caused by electron injection. Energetics of adsorbed hydrogen at the p-gallium arsenide electrode. Journal of the American Chemical Society, 1986, 108, 4294-4298.	13.7	71
62	Two-Dimensional Chirality:  Self-Assembled Monolayer of an Atropisomeric Compound Covalently Bound to a Gold Surface. Journal of the American Chemical Society, 1999, 121, 6515-6516.	13.7	71
63	Formation of Self-Assembled Monolayers of Alkanethiols on GaAs Surface with in Situ Surface Activation by Ammonium Hydroxide. Langmuir, 1999, 15, 8577-8579.	3.5	71
64	Unidirectional Electron Transfer at Self-Assembled Monolayers of 11-Ferrocenyl-1-undecanethiol on Gold. Bulletin of the Chemical Society of Japan, 1993, 66, 1032-1037.	3.2	69
65	Coverage dependent behavior of redox reaction induced structure change and mass transport at an 11-ferrocenyl-1-undecanethiol self-assembled monolayer on a gold electrode studied by an in situ IRRAS–EQCM combined system. Physical Chemistry Chemical Physics, 1999, 1, 3653-3659.	2.8	68
66	Electrochemical Control of the Second Harmonic Generation Property of Self-Assembled Monolayers Containing atrans-Ferrocenyl-Nitrophenyl Ethylene Group on Gold. Journal of the American Chemical Society, 1999, 121, 391-398.	13.7	68
67	Two-Dimensional Crystals of Alkanes Formed on Au(111) Surface in Neat Liquid:Â Structural Investigation by Scanning Tunneling Microscopy. Journal of Physical Chemistry B, 2000, 104, 6021-6027.	2.6	68
68	Polarization Modulation Fourier Transform Infrared Studies of the Effects of Self-Assembly Time on the Order and Orientation of 11-Ferrocenyl-1-undecanethiol Monolayers on Gold. Bulletin of the Chemical Society of Japan, 1994, 67, 21-25.	3.2	67
69	Electrochemical in situ FT-IRRAS studies of a self-assembled monolayer of 2-(11-mercaptoundecyl)hydroquinone. Journal of the Chemical Society, Faraday Transactions, 1996, 92, 3813.	1.7	67
70	Unfolding, Aggregation, and Amyloid Formation by the Tetramerization Domain from Mutant p53 Associated with Lung Cancerâ€. Biochemistry, 2006, 45, 1608-1619.	2.5	67
71	Lithium-metal deposition/dissolution within internal space of CNT 3D matrix results in prolonged cycle of lithium-metal negative electrode. Carbon, 2017, 119, 119-123.	10.3	67
72	Effects of the Helmholtz Layer Capacitance on the Potential Distribution at Semiconductor/Electrolyte Interface and the Linearity of the Mottâ€Schottky Plot. Journal of the Electrochemical Society, 1983, 130, 895-897.	2.9	66

#	Article	IF	CITATIONS
73	Recent progress in liquid electrolytes for lithium metal batteries. Current Opinion in Electrochemistry, 2019, 17, 106-113.	4.8	66
74	Simultaneous detection of structural change and mass transport accompanying the redox of a ferrocenylundecanethiol monolayer with the novel FT-IR reflection absorption spectroscopy/electrochemical quartz crystal microbalance combined system. Journal of Electroanalytical Chemistry, 1994, 375, 409-413.	3.8	64
75	An In Situ Electrochemical Quartz Crystal Microbalance Study of the Dissolution Process of a Gold Electrode in Perchloric Acid Solution Containing Chloride Ion. Journal of the Electrochemical Society, 1998, 145, 1614-1623.	2.9	64
76	Mechanism for nucleation and growth of electrochemical palladium deposition on an Au(111) electrode. Journal of Electroanalytical Chemistry, 2002, 520, 126-132.	3.8	64
77	Enhancement of SERS Background through Charge Transfer Resonances on Single Crystal Gold Surfaces of Various Orientations. Journal of the American Chemical Society, 2013, 135, 17387-17392.	13.7	64
78	Formation and characterization of thiol-derivatized zinc (II) porphyrin monolayers on gold. Thin Solid Films, 1996, 273, 250-253.	1.8	63
79	Epitaxial growth of a palladium layer on an Au(100) electrode. Journal of Electroanalytical Chemistry, 1999, 473, 2-9.	3.8	63
80	Characterization of self-assembled monolayers of alkanethiol on GaAs surface by contact angle and angle-resolved XPS measurements. Surface Science, 2003, 529, 163-170.	1.9	63
81	Evidence of Nonelectrochemical Shift Reaction on a CO-Tolerant High-Entropy State Pt–Ru Anode Catalyst for Reliable and Efficient Residential Fuel Cell Systems. Journal of the American Chemical Society, 2012, 134, 14508-14512.	13.7	63
82	Preparative method for fabricating a microelectrode ensemble: electrochemical response of microporous aluminum anodic oxide film modified gold electrode. Analytical Chemistry, 1990, 62, 652-656.	6.5	62
83	Layer-by-layer self-assembly of composite films of CdS nanoparticle and alkanedithiol on gold: an X-ray photoelectron spectroscopic characterization. Chemical Physics Letters, 1997, 278, 233-237.	2.6	62
84	Post-assembly insertion of metal ions into thiol-derivatized porphyrin monolayers on gold. Journal of Electroanalytical Chemistry, 1999, 473, 75-84.	3.8	62
85	In situ structural study on underpotential deposition of Ag on Au(111) electrode using surface X-ray scattering technique. Journal of Electroanalytical Chemistry, 2002, 532, 201-205.	3.8	61
86	Electrochemical Oxidative Formation and Reductive Desorption of a Self-Assembled Monolayer of Decanethiol on a Au(111) Surface in KOH Ethanol Solution. Journal of Physical Chemistry B, 2004, 108, 6422-6428.	2.6	61
87	Solvent Effect on the Structure of the Self-Assembled Monolayer of Alkanethiol. Chemistry Letters, 1999, 28, 667-668.	1.3	60
88	Electron Transfer through Organic Monolayers Directly Bonded to Silicon Probed by Current Sensing Atomic Force Microscopy:Â Effect of Chain Length and Applied Force. Journal of Physical Chemistry B, 2004, 108, 17129-17135.	2.6	58
89	Electrochemical Metal Deposition on Top of an Organic Monolayer. Journal of Physical Chemistry B, 2006, 110, 17570-17577.	2.6	56
90	Decomposition Processes of an Organic Monolayer Formed on Si(111) via a SiliconCarbon Bond Induced by Exposure to UV Irradiation or Ozone. Langmuir, 2004, 20, 1207-1212.	3.5	55

#	Article	IF	CITATIONS
91	Electrocatalytic activity of various types of h-BN for the oxygen reduction reaction. Physical Chemistry Chemical Physics, 2014, 16, 13755-13761.	2.8	55
92	Structure of Pt microparticles dispersed electrochemically onto glassy carbon electrodes. Journal of Electroanalytical Chemistry and Interfacial Electrochemistry, 1988, 256, 481-487.	0.1	54
93	pH-dependent photoinduced electron transfer at the gold electrode modified with a self-assembled monolayer of a porphyrin-mercaptoquinone coupling molecule. Journal of Electroanalytical Chemistry, 1997, 438, 121-126.	3.8	54
94	Microscopic Electrode Processes in the Four-Electron Oxygen Reduction on Highly Active Carbon-Based Electrocatalysts. ACS Catalysis, 2018, 8, 8162-8176.	11.2	54
95	Determination of Thickness of a Self-Assembled Monolayer of Dodecanethiol on Au(111) by Angle-Resolved X-ray Photoelectron Spectroscopy. Langmuir, 1998, 14, 5656-5658.	3.5	52
96	Electrochemical Control of CO/NO Ligand Exchange in a Triruthenium Cluster Monolayer Assembled on a Gold Electrode Surface. Journal of the American Chemical Society, 2004, 126, 7434-7435.	13.7	52
97	Evidence for Epitaxial Arrangement and High Conformational Order of an Organic Monolayer on Si(111) by Sum Frequency Generation Spectroscopy. Journal of the American Chemical Society, 2004, 126, 7034-7040.	13.7	52
98	Plasmonic Enhancement of Photoinduced Uphill Electron Transfer in a Molecular Monolayer System. Angewandte Chemie - International Edition, 2011, 50, 1280-1284.	13.8	52
99	A self-assembled monolayer of ferrocenylalkane thiols on gold as an electron mediator for the reduction of Fe(III)-EDTA in solution. Electrochimica Acta, 1991, 36, 1799-1801.	5.2	51
100	Angle-Resolved X-Ray Photoelectron Spectroscopic Study on a Self-Assembled Monolayer of a Porphyrin–Ferrocene–Thiol Linked Molecule on Gold: Evidence for a Highly Ordered Arrangement for Efficient Photoinduced Electron Transfer. Bulletin of the Chemical Society of Japan, 1998, 71, 2555-2559.	3.2	51
101	Dielectric properties of organic monolayers directly bonded on silicon probed by current sensing atomic force microscope. Applied Physics Letters, 2003, 83, 2034-2036.	3.3	51
102	Subnanoscale hydrophobic modulation of salt bridges in aqueous media. Science, 2015, 348, 555-559.	12.6	51
103	Surface Mass Titrations of Self-Assembled Monolayers of ω-Mercaptoalkanoic Acids on Gold. Chemistry Letters, 1998, 27, 669-670.	1.3	50
104	Synthesis, Structure, and Second-Harmonic Generation of Noncentrosymmetric Cocrystals of 2-Amino-5-nitropyridine with Achiral Benzenesulfonic Acids. Crystal Growth and Design, 2001, 1, 467-471.	3.0	50
105	Electron and ion transfer through multilayers of gold nanoclusters covered by self-assembled monolayers of alkylthiols with various functional groups. Faraday Discussions, 2002, 121, 373-389.	3.2	50
106	Evaluation of electron-hole recombination properties of titanium (IV) oxide particles with high photocatalytic activity. Research on Chemical Intermediates, 2007, 33, 285-296.	2.7	50
107	Electrochemical and in situ FTIR studies of ethanol adsorption and oxidation on gold single crystal electrodes in alkaline media. Journal of Electroanalytical Chemistry, 2013, 707, 89-94.	3.8	50
108	Two-Dimensional Corrugated Porous Carbon-, Nitrogen-Framework/Metal Heterojunction for Efficient Multielectron Transfer Processes with Controlled Kinetics. ACS Nano, 2017, 11, 1770-1779.	14.6	50

#	Article	IF	CITATIONS
109	Absorption behaviour of 4,4′-bipyridyl at a gold/water interface and its role in the electron transfer reaction between cytochrome c and a gold electrode. Journal of Electroanalytical Chemistry and Interfacial Electrochemistry, 1981, 122, 321-326.	0.1	49
110	Attenuated total reflection Fourier transform infrared spectroscopy study of the adsorption of organic contaminants on a hydrogen-terminated Si(111) surface in air. Applied Physics Letters, 1999, 75, 1562-1564.	3.3	49
111	Molecular structure at electrode/electrolyte solution interfaces related to electrocatalysis. Faraday Discussions, 2008, 140, 125-137.	3.2	49
112	Potential-Dependent Structures and Potential-Induced Structure Changes at Pt(111) Single-Crystal Electrode/Sulfuric and Perchloric Acid Interfaces in the Potential Region between Hydrogen Underpotential Deposition and Surface Oxide Formation by <i>In Situ</i> Surface X-ray Scattering. Journal of Physical Chemistry C, 2016, 120, 16118-16131.	3.1	49
113	The photoelectrochemical behaviour of electrochemically deposited CdTe films. Electrochimica Acta, 1984, 29, 279-281.	5.2	48
114	Packing State and Stability of Self-Assembled Monolayers of 11-Ferrocenyl-1-undecanethiol on Platinum Electrodes. Bulletin of the Chemical Society of Japan, 1994, 67, 863-865.	3.2	48
115	Photoelectrochemical characteristics of a self-assembled monolayer of porphyrin-mercaptoquinone coupling molecules. Thin Solid Films, 1996, 284-285, 652-655.	1.8	48
116	Porous gold nanodisks with multiple internal hot spots. Physical Chemistry Chemical Physics, 2012, 14, 9131.	2.8	48
117	Potential-Dependent Adsorption and Desorption of Perfluorosulfonated Ionomer on a Platinum Electrode Surface Probed by Electrochemical Quartz Crystal Microbalance and Atomic Force Microscopy. Journal of Physical Chemistry C, 2013, 117, 15704-15709.	3.1	48
118	Potential Dependent Orientation and Oxidative Decomposition of Mercaptoalkanenitrile Monolayers on Gold. An in Situ Fourier Transform Infrared Spectroscopy Study. Langmuir, 1996, 12, 2726-2736.	3.5	47
119	Electrochemical deposition of palladium on an Au(111) electrode: effects of adsorbed hydrogen for a growth mode. Colloids and Surfaces A: Physicochemical and Engineering Aspects, 1999, 154, 201-208.	4.7	47
120	Electrochemical oxidative adsorption and reductive desorption of a self-assembled monolayer of decanethiol on the Au(111) surface in KOH+ethanol solution. Journal of Electroanalytical Chemistry, 2003, 550-551, 321-325.	3.8	47
121	Sum frequency generation study on the molecular structures at the interfaces between quartz modified with amino-terminated self-assembled monolayer and electrolyte solutions of various pH and ionic strengths. Electrochimica Acta, 2001, 46, 3057-3061.	5.2	46
122	Self-assembled monolayers (SAMs) with photo-functionalities. Journal of Photochemistry and Photobiology C: Photochemistry Reviews, 2007, 8, 1-17.	11.6	46
123	On-line spectral estimation of nonstationary time series based on AR model parameter estimation and order selection with a forgetting factor. IEEE Transactions on Signal Processing, 1995, 43, 1519-1522.	5.3	45
124	Selfâ€Assembled Monolayers of Compact Phosphanes with Alkanethiolate Pendant Groups: Remarkable Reusability and Substrate Selectivity in Rh Catalysis. Angewandte Chemie - International Edition, 2008, 47, 5627-5630.	13.8	45
125	Metal Cation-Induced Deformation of DNA Self-Assembled Monolayers on Silicon: Vibrational Sum Frequency Generation Spectroscopy. Journal of the American Chemical Society, 2008, 130, 8016-8022.	13.7	45
126	Spectroscopic Studies on Electroless Deposition of Copper on a Hydrogen-Terminated Si(111) Surface in Fluoride Solutions. Journal of the Electrochemical Society, 2001, 148, C421.	2.9	44

#	Article	IF	CITATIONS
127	Enantioselective Adsorption of Phenylalanine onto Self-Assembled Monolayers of 1,1â€~-Binaphthalene-2,2â€~-dithiol on Gold. Journal of the American Chemical Society, 2002, 124, 740-741.	13.7	44
128	Conductivity of Nation membranes at low temperatures. Journal of Electroanalytical Chemistry and Interfacial Electrochemistry, 1990, 287, 163-169.	0.1	43
129	Characterization of Silicon Carbide-Silicon Nitride Composite Ultrafine Particles Synthesized Using a CO2 Laser by Silicon-29 Magic Angle Spinning NMR and ESR. Journal of the American Ceramic Society, 1995, 78, 83-89.	3.8	43
130	SFG study on potential-dependent structure of water at Pt electrode/electrolyte solution interface. Electrochimica Acta, 2008, 53, 6841-6844.	5.2	43
131	The Theory of the Lightâ€Induced Evolution of Hydrogen at Semiconductor Electrodes. Journal of the Electrochemical Society, 1978, 125, 223-227.	2.9	42
132	In situ optical second harmonic generation studies of electrochemical deposition of tellurium on polycrystalline gold electrodes. Journal of Electroanalytical Chemistry, 1996, 401, 95-101.	3.8	42
133	Reaction pathway of four-electron oxidation of formaldehyde on platinum electrode as observed by in situ optical spectroscopy. Surface Science, 1997, 386, 82-88.	1.9	42
134	Effects of Alkylchain Length on the Efficiency of Photoinduced Electron Transfer at Gold Electrodes Modified with Self-Assembled Monolayers of Molecules Containing Porphyrin, Ferrocene and Thiol Separated each other by Alkylchains. Zeitschrift Fur Physikalische Chemie, 1999, 212, 23-30.	2.8	42
135	Photoexcited Hole Transfer to a MnOxCocatalyst on a SrTiO3Photoelectrode during Oxygen Evolution Studied by In Situ X-ray Absorption Spectroscopy. Journal of Physical Chemistry C, 2014, 118, 24302-24309.	3.1	42
136	In-situ FT-IR Spectroelectrochemical Study of the Trinuclear Complex [Ru3(.mu.3-O)(.muCH3COO)6(CO)(pyridine)2] in Acetonitrile. Inorganic Chemistry, 1995, 34, 4527-4528.	4.0	41
137	Stability of the Si–H bond on the hydrogen-terminated Si(111) surface studied by sum frequency generation. Surface Science, 2001, 476, 121-128.	1.9	41
138	Composition and electronic properties of electrochemically deposited CdTe films. Journal of Applied Physics, 1984, 55, 3879-3881.	2.5	40
139	In-situ, real time monitoring of electrode surfaces by scanning tunneling microscopy. Journal of Electroanalytical Chemistry and Interfacial Electrochemistry, 1989, 259, 301-308.	0.1	40
140	Anion effect on the electrochemical characteristics of a gold electrode modified with a self-assembled monolayer of ferrocenylhexanethiol in aqueous and dichloromethane solutions. Journal of Organometallic Chemistry, 2001, 637-639, 841-844.	1.8	40
141	Oxidation States and CO Ligand Exchange Kinetics in a Self-Assembled Monolayer of a Triruthenium Cluster Studied by In Situ Infrared Spectroscopy. Chemistry - A European Journal, 2005, 11, 5040-5054.	3.3	40
142	Structure of water at zwitterionic copolymer film–liquid water interfaces as examined by the sum frequency generation method. Colloids and Surfaces B: Biointerfaces, 2014, 113, 361-367.	5.0	40
143	Study of the Fe(CN)3â^'6/Fe(CN)4â^'6 redox system on Pt by EMIRS. Journal of Electroanalytical Chemistry and Interfacial Electrochemistry, 1989, 262, 195-209.	0.1	39
144	Cobalt phthalocyanine analogs as soluble catalysts that improve the charging performance of Li-O2 batteries. Chemical Physics Letters, 2015, 620, 78-81.	2.6	39

#	Article	IF	CITATIONS
145	Hyper-Raman scattering enhanced by anisotropic dimer plasmons on artificial nanostructures. Journal of Chemical Physics, 2007, 127, 111103.	3.0	38
146	Quantum-to-Classical Transition of Proton Transfer in Potential-Induced Dioxygen Reduction. Physical Review Letters, 2018, 121, 236001.	7.8	38
147	Resistivity, carrier concentration, and carrier mobility of electrochemically deposited CdTe films. Journal of Applied Physics, 1986, 60, 2046-2049.	2.5	37
148	A Novel Nanolithography Technique for Self-Assembled Monolayers Using a Current Sensing Atomic Force Microscope. Langmuir, 2001, 17, 7784-7788.	3.5	37
149	Crystal-face specific response of a single-crystal cadmium sulfide based ion-selective electrode. Analytical Chemistry, 1989, 61, 1980-1983.	6.5	36
150	In Situ Dynamic Monitoring of Electrochemical Oxidative Adsorption and Reductive Desorption Processes of a Self-Assembled Monolayer of Hexanethiol on a Au(111) Surface in KOH Ethanol Solution by Scanning Tunneling Microscopy. Langmuir, 2005, 21, 4024-4033.	3.5	36
151	Interfacial electron transfer as a significant step in photoelectrochemical reactions on some semiconductors. Journal of Applied Physics, 1981, 52, 808-810.	2.5	35
152	Electrochemical Deposition, Optical Properties, and Photoelectrochemical Behavior of CdTe Films. Journal of the Electrochemical Society, 1984, 131, 2304-2307.	2.9	35
153	Adsorption of Hexachloroplatinate Complex on Au(111) Electrode. Anin SituScanning Tunneling Microscopy and Electrochemical Quartz Microbalance Study. Langmuir, 1997, 13, 594-596.	3.5	35
154	Monitoring Electron Transfer in an Azobenzene Self-Assembled Monolayer byin SituInfrared Reflection Absorption Spectroscopy. Langmuir, 1998, 14, 619-624.	3.5	35
155	A novel spectroelectrochemical cell for in situ surface X-ray scattering measurements of single crystal disk electrodes. Electrochimica Acta, 2002, 47, 3075-3080.	5.2	35
156	Electron and ion transport through multilayers of Au nanoclusters covered by self-assembled monolayers. Journal of Electroanalytical Chemistry, 2003, 554-555, 385-393.	3.8	35
157	Substrate dependent structure of adsorbed aryl isocyanides studied by sum frequency generation (SFC) spectroscopy. Physical Chemistry Chemical Physics, 2010, 12, 3156.	2.8	35
158	Gold nanoparticle decoration of insulating boron nitride nanosheet on inert gold electrode toward an efficient electrocatalyst for the reduction of oxygen to water. Electrochemistry Communications, 2016, 66, 53-57.	4.7	35
159	Carbon-black-based self-standing porous electrode for 500 Wh/kg rechargeable lithium-oxygen batteries. Cell Reports Physical Science, 2021, 2, 100506.	5.6	35
160	Surface Functionalization of Doped CVD Diamond via Covalent Bond. An XPS Study on the Formation of Surface-bound Quaternary Pyridinium Salt. Chemistry Letters, 1998, 27, 953-954.	1.3	34
161	A rotating gold ring–gold disk electrode study on electrochemical reductive desorption and oxidative readsorption of a self-assembled monolayer of dodecanethiol. Journal of Electroanalytical Chemistry, 2002, 538-539, 59-63.	3.8	34
162	Interfacial water structure at polymer gel/quartz interfaces investigated by sum frequency generation spectroscopy. Physical Chemistry Chemical Physics, 2008, 10, 4987.	2.8	34

#	Article	IF	CITATIONS
163	Potential-Dependent Adsorption/Desorption Behavior of Perfluorosulfonated Ionomer on a Gold Electrode Surface Studied by Cyclic Voltammetry, Electrochemical Quartz Microbalance, and Electrochemical Atomic Force Microscopy. Langmuir, 2013, 29, 2420-2426.	3.5	34
164	Adsorption and Catalytic Activation of the Molecular Oxygen on the Metal Supported h-BN. Topics in Catalysis, 2014, 57, 1032-1041.	2.8	34
165	Anion Adsorption on Gold Electrodes Studied by Electrochemical Surface Forces Measurement. Journal of Physical Chemistry C, 2016, 120, 15986-15992.	3.1	34
166	Effects of contaminant water on coulombic efficiency of lithium deposition/dissolution reactions in tetraglyme-based electrolytes. Journal of Power Sources, 2017, 350, 73-79.	7.8	34
167	Electrochemical impedance analysis of the Li/Au-Li7La3Zr2O12 interface during Li dissolution/deposition cycles: Effect of pre-coating Li7La3Zr2O12 with Au. Journal of Electroanalytical Chemistry, 2019, 835, 143-149.	3.8	33
168	Photoluminescence and impedance study of p-gallium arsenide/electrolyte interfaces under cathodic bias: evidence for flat-band potential shift during illumination and introduction of high-density surface states by platinum treatment. The Journal of Physical Chemistry, 1989, 93, 6521-6526.	2.9	32
169	In Situ Infrared Spectroscopic Studies of Adsorption of Lactic Acid and Related Compounds on the TiO2and CdS Semiconductor Photocatalyst Surfaces from Aqueous Solutions. Chemistry Letters, 1998, 27, 849-850.	1.3	32
170	Functionalization of silicon surfaces with catalytically active Pd complexes and application to the aerobic oxidation of benzylic alcohols. Chemical Communications, 2007, , 4280.	4.1	32
171	In situ observation of carrier transfer in the Mn-oxide/Nb:SrTiO3 photoelectrode by X-ray absorption spectroscopy. Chemical Communications, 2013, 49, 7848.	4.1	32
172	Nonlinear Iron Electrochemical Oscillator: Coupling and Photo Effects. Journal of the Electrochemical Society, 1996, 143, 2258-2262.	2.9	31
173	Effect of Surface Morphology of a Gold Substrate on Photocurrent Efficiency at a Gold Electrode Modified with a Self-Assembled Monolayer of a Porphyrin–Ferrocene–Thiol Linked Molecule. Chemistry Letters, 2000, 29, 964-965.	1.3	31
174	Characterization of novel redox-active triruthenium(III) complexes with a disulfide alkyl ligand. Anion-dependent redox behaviour of monolayer assemblies on gold â€. Dalton Transactions RSC, 2000, , 2693-2702.	2.3	31
175	Gap-mode SERS studies of azobenzene-containing self-assembled monolayers on Au(111). Journal of Colloid and Interface Science, 2010, 341, 366-375.	9.4	31
176	1,6-Hexanedithiol Self-Assembled Monolayers on Au(111) Investigated by Electrochemical, Spectroscopic, and Molecular Mechanics Methods. Journal of Physical Chemistry C, 2010, 114, 497-505.	3.1	31
177	Structural Study of Electrochemically Deposited Cu on p-GaAs(100) in H2SO4 Solution by In Situ Surface-Sensitive X-ray Absorption Fine Structure Measurements. Journal of Physical Chemistry B, 2000, 104, 9017-9024.	2.6	30
178	Hydrophilicity transition of the clean rutile TiO2 (1 1 0) surface. Electrochimica Acta, 2008, 53, 6173-6177.	5.2	30
179	Going beyond the self-assembled monolayer: metal intercalated dithiol multilayers and their conductance. RSC Advances, 2014, 4, 39657-39666.	3.6	30
180	Potassium Ions Promote Solution-Route Li ₂ O ₂ Formation in the Positive Electrode Reaction of Li–O ₂ Batteries. Journal of Physical Chemistry Letters, 2017, 8, 1142-1146.	4.6	30

#	Article	IF	CITATIONS
181	Structure Dependence of the Surface p <i>Ka</i> of Mercaptoundecanoic Acid SAM on Gold. Electrochemistry, 1999, 67, 1172-1174.	1.4	30
182	Construction of Semiconductor Nanoparticle Layers on Gold by Self-Assembly Technique. Japanese Journal of Applied Physics, 1997, 36, 4053-4056.	1.5	29
183	Photoconversion of a Redox-Active Self-Assembled Monolayer: In Situ Probing of Photoinduced CO Dissociation from a Triruthenium Cluster Center on Gold. Angewandte Chemie - International Edition, 2005, 44, 416-419.	13.8	29
184	Formation and Structure of Perfluorosulfonated Ionomer Thin Film on a Graphite Surface. Chemistry Letters, 2009, 38, 884-885.	1.3	29
185	Surface-enhanced Raman scattering at well-defined single crystalline faces of platinum-group metals induced by gap-mode plasmon excitation. Journal of Photochemistry and Photobiology A: Chemistry, 2011, 221, 175-180.	3.9	29
186	Structural Tuning of Optical Antenna Properties for Plasmonic Enhancement of Photocurrent Generation on a Molecular Monolayer System. Journal of Physical Chemistry C, 2012, 116, 20806-20811.	3.1	29
187	Structure and Photoelectrochemical Properties of Laminated Monoparticle Layers of CdS and ZnS on Gold. Japanese Journal of Applied Physics, 1999, 38, 518-521.	1.5	28
188	Molecular Orientation and Electrochemical Stability of Azobenzene Self-Assembled Monolayers on Gold:Â An In-Situ FTIR Study. Langmuir, 2000, 16, 6948-6954.	3.5	28
189	A ligand substitution reaction of oxo-centred triruthenium complexes assembled as monolayers on gold electrodes. Physical Chemistry Chemical Physics, 2001, 3, 3420-3426.	2.8	28
190	Resonance Hyper-Raman Scattering of Fullerene C60 Microcrystals. Journal of Physical Chemistry A, 2008, 112, 790-793.	2.5	28
191	Cathodes For Photodriven Hydrogen Generators: Znte and Cdte. International Journal of Energy Research, 1977, 1, 25-30.	4.5	27
192	Mechanistic Study of Photoelectrochemical Reactions at a p â€â€‰GaP Electrode. Journal of the Electrochemical Society, 1981, 128, 2153-2158.	2.9	27
193	Simultaneous UV-Vis spectroelectrochemical and quartz crystal microgravimetric measurements during the redox reaction of viologens. Journal of Electroanalytical Chemistry, 1993, 350, 321-327.	3.8	27
194	<i>In situ</i> Real-time Monitoring of Electrochemical Ag Deposition on a Reconstructed Au(111) Surface Studied by Scanning Tunneling Microscopy. Journal of Physical Chemistry C, 2008, 112, 3073-3077.	3.1	27
195	Water Structure at Superhydrophobic Quartz/Water Interfaces: A Vibrational Sum Frequency Generation Spectroscopy Study. Journal of Physical Chemistry C, 2009, 113, 21155-21161.	3.1	27
196	Structure of water in the vicinity of a zwitterionic polymer brush as examined by sum frequency generation method. Colloids and Surfaces B: Biointerfaces, 2012, 100, 126-132.	5.0	27
197	Plasmonically Nanoconfined Light Probing Invisible Phonon Modes in Defect-Free Graphene. Journal of the American Chemical Society, 2013, 135, 11489-11492.	13.7	27
198	An electrochemical AFM study on electrodeposition of copper on p-GaAs(100) surface in HCl solution. Electrochimica Acta, 1995, 40, 1345-1351.	5.2	26

#	Article	IF	CITATIONS
199	Dissociative adsorption dynamics of formaldehyde on a platinum electrode surface; one-dimensional domino?. Chemical Physics, 1996, 205, 269-275.	1.9	26
200	Local structures of isovalent and heterovalent dilute impurities in Si crystal probed by fluorescence x-ray absorption fine structure. Journal of Applied Physics, 1997, 82, 4810-4815.	2.5	26
201	Excitation Wavelength Dependent Three-Wave Mixing at a CO-Covered Platinum Electrode. Journal of Physical Chemistry B, 1997, 101, 7414-7421.	2.6	26
202	Nonlinear state estimation by evolution strategies based particle filters. , 0, , .		26
203	Effects of concentration and temperature on the formation process of decanethiol self-assembled monolayer on Au(111) followed by electrochemical reductive desorption. Electrochimica Acta, 2008, 53, 6196-6201.	5.2	26
204	Criteria for evaluating lithium–air batteries in academia to correctly predict their practical performance in industry. Materials Horizons, 2022, 9, 856-863.	12.2	26
205	Optimal input design for autoregressive model discrimination with constrained output variance. IEEE Transactions on Automatic Control, 1984, 29, 348-350.	5.7	25
206	Effects of heat treatment on the composition and semiconductivity of electrochemically deposited CdTe films. Journal of Applied Physics, 1985, 58, 4292-4295.	2.5	25
207	In Situ Optical Second Harmonic Rotational Anisotropy Measurements of an Au(111) Electrode during Electrochemical Deposition of Tellurium. Journal of Physical Chemistry B, 1998, 102, 2677-2683.	2.6	25
208	Structure and Reactivity of Alkoxycarbonyl (Ester)-Terminated Monolayers on Silicon:Â Sum Frequency Generation Spectroscopy. Journal of Physical Chemistry B, 2006, 110, 4892-4899.	2.6	25
209	Stability of underpotentially deposited Ag layers on a Au(111) surface studied by surface X-ray scattering. Electrochemistry Communications, 2009, 11, 804-807.	4.7	25
210	Coherent Phonon Dynamics in Single-Walled Carbon Nanotubes Studied by Time-Frequency Two-Dimensional Coherent Anti-Stokes Raman Scattering Spectroscopy. Nano Letters, 2009, 9, 1378-1381.	9.1	25
211	Resonance surface X-ray scattering technique to determine the structure of electrodeposited Pt ultrathin layers on Au(111) surface. Electrochimica Acta, 2010, 55, 8302-8306.	5.2	25
212	Humidity-Dependent Structure of Surface Water on Perfluorosulfonated Ionomer Thin Film Studied by Sum Frequency Generation Spectroscopy. Journal of Physical Chemistry C, 2010, 114, 3958-3961.	3.1	25
213	Interfacial Molecular Structures of Polyelectrolyte Brush in Contact with Dry Nitrogen, Water Vapor, Liquid Water, and Aqueous Electrolyte Solution Studied by Sum Frequency Generation Spectroscopy. Journal of the American Chemical Society, 2010, 132, 17271-17276.	13.7	25
214	Terpyridine platinum(ii) complexes containing triazine di- or tri-thiolate bridges: structures, luminescence, electrochemistry, and aggregation. Dalton Transactions, 2012, 41, 11497.	3.3	25
215	Electronic Structure of the CO/Pt(111) Electrode Interface Probed by Potential-Dependent IR/Visible Double Resonance Sum Frequency Generation Spectroscopy. Journal of Physical Chemistry C, 2015, 119, 26056-26063.	3.1	25
216	Vibrational Spectroscopic Observation of Atomic-Scale Local Surface Sites Using Site-Selective Signal Enhancement. Nano Letters, 2015, 15, 7982-7986.	9.1	25

#	Article	IF	CITATIONS
217	Highly Efficient Oxygen and Hydrogen Electrocatalytic Activities of Selfâ€Morphogenic Nanoporous Carbon, Nitrogen Architectures. ChemNanoMat, 2016, 2, 99-103.	2.8	25
218	Improved Energy Capacity of Aprotic Li–O ₂ Batteries by Forming Cl-Incorporated Li ₂ O ₂ as the Discharge Product. Journal of Physical Chemistry C, 2016, 120, 13360-13365.	3.1	25
219	Effect of Electrolyte Concentration on the Solvation Structure of Gold/LITFSI–DMSO Solution Interface. Journal of Physical Chemistry C, 2020, 124, 12381-12389.	3.1	25
220	Structural Investigation of the Self-Assembled Monolayer of Decanethiol on the Reconstructed and (1×1)-Au(100) Surfaces by Scanning Tunneling Microscopy. Langmuir, 2001, 17, 4148-4150.	3.5	24
221	Sum frequency generation study on the structure of water in the vicinity of an amphoteric polymer brush. Colloids and Surfaces B: Biointerfaces, 2012, 91, 215-218.	5.0	24
222	Formation of Functionalized Nanowires by Control of Selfâ€Assembly Using Multiple Modified Amyloid Peptides. Advanced Functional Materials, 2013, 23, 4881-4887.	14.9	24
223	The Stability of Photoelectrodes. Journal of the Electrochemical Society, 1977, 124, 98-99.	2.9	23
224	AFM tip induced selective electrochemical etching of and metal deposition on p-GaAs(100) surface. Surface Science, 1996, 357-358, 565-570.	1.9	23
225	Construction and electrochemical characteristics of multilayer assemblies of Au nanoclusters protected by mixed self-assembled monolayers on tin-doped indium oxide. Physical Chemistry Chemical Physics, 2003, 5, 5279.	2.8	23
226	Electrochemical Assembly and Potential-Dependent Plasmon Absorption of Au Nanoclusters Covered with a 4-Aminothiophenol Self-Assembled Monolayer. Journal of Physical Chemistry B, 2005, 109, 9897-9904.	2.6	23
227	Photoinduced Surface Dynamics of CO Adsorbed on a Platinum Electrode. Journal of Physical Chemistry B, 2006, 110, 15055-15058.	2.6	23
228	Surface Coordination of Nitric Oxide to a Self-Assembled Monolayer of a Triruthenium Cluster: An in Situ Infrared Spectroscopic Study. Langmuir, 2008, 24, 8027-8035.	3.5	23
229	Effect of Electrolyte Filling Technology on the Performance of Porous Carbon Electrode-Based Lithium-Oxygen Batteries. ACS Applied Energy Materials, 2021, 4, 2563-2569.	5.1	23
230	In-situ and real time monitoring of the InSe surface by atomic force microscopy with atomic resolution during electrochemical reactions. Journal of Electroanalytical Chemistry, 1993, 357, 301-306.	3.8	22
231	Formation of Organic Monolayer on a Hydrogen Terminated Si(111) SurfaceviaSilicon-Carbon Bond Monitored by ATR FT-IR and SFG Spectroscopy: Effect of Orientational Order on the Reaction Rate. Chemistry Letters, 2002, 31, 208-209.	1.3	22
232	Highly-Sensitive Determination of 6-Mercaptopurine and Its Metabolites by Electrochemical Reductive Desorption Measurements. Electroanalysis, 2005, 17, 965-968.	2.9	22
233	Fabrication of photochemical pattern on a self-assembled monolayer (SAM) of a ruthenium cluster under electrochemical control. Journal of Materials Chemistry, 2009, 19, 261-267.	6.7	22
234	Molecular Catalysts Confined on and Within Molecular Layers Formed on a Si(111) Surface with Direct Si–C Bonds. Advanced Materials, 2012, 24, 268-272.	21.0	22

#	Article	IF	CITATIONS
235	Structure of Pt(111)/lonomer Membrane Interface and Its Bias-Induced Change in Membrane Electrode Assembly. Journal of Physical Chemistry C, 2013, 117, 12168-12171.	3.1	22
236	Nanoscale Optical and Mechanical Manipulation of Molecular Alignment in Metal–Molecule–Metal Structures. Journal of Physical Chemistry C, 2014, 118, 21550-21557.	3.1	22
237	Structural Study of Electrochemically Lithiated Si(111) by using Soft Xâ€ray Emission Spectroscopy Combined with Scanning Electron Microscopy and through Xâ€ray Diffraction Measurements. ChemElectroChem, 2016, 3, 959-965.	3.4	22
238	An efficient electrocatalyst for oxygen reduction to water - boron nitride nanosheets decorated with small gold nanoparticles (~ 5 nm) of narrow size distribution on gold substrate. Journal of Electroanalytical Chemistry, 2018, 819, 107-113.	3.8	22
239	In situ, realâ€time monitoring of electrode surfaces by scanning tunneling microscopy. III. Surface structure of Pt and Pd electrodes. Journal of Vacuum Science and Technology A: Vacuum, Surfaces and Films, 1990, 8, 520-524.	2.1	21
240	Synthesis and electrochemical characterization of self-assembled monolayers of redox-active oxide-bridged triruthenium(III) clusters on Au(111). Journal of Electroanalytical Chemistry, 1999, 473, 93-98.	3.8	21
241	pH-Dependent Water Structure at a Quartz Surface Modified with an Amino-Terminated Monolayer Studied by Sum Frequency Generation (SFG). Chemistry Letters, 2000, 29, 734-735.	1.3	21
242	Construction of Mono- and Multimolecular Layers with Electron Transfer Mediation Function and Catalytic Activity for Hydrogen Evolution on a Hydrogen-Terminated Si(111) Surface via Siâ^'C Bond. Journal of Physical Chemistry C, 2008, 112, 10923-10930.	3.1	21
243	Examination of the electroactive composites containing cobalt nanoclusters and nitrogen-doped nanostructured carbon as electrocatalysts for oxygen reduction reaction. Journal of Power Sources, 2012, 220, 20-30.	7.8	21
244	In situ real-time study on potential induced structure change at Au(111) and Au(100) single crystal electrode/sulfuric acid solution interfaces by surface x-ray scattering. Surface Science, 2015, 631, 96-104.	1.9	21
245	Photoelectrochemical Production of Hydrogen. Advances in Chemistry Series, 1977, , 33-70.	0.6	20
246	Novel application of scanning tunneling microscopy — tip current voltammetry of n-GaAs and p-GaP in electrolyte solution. Surface Science, 1990, 237, 280-290.	1.9	20
247	Xâ€ray photoelectron spectroscopic studies of the chemical nature of asâ€prepared and NaOHâ€treated porous silicon layer. Applied Physics Letters, 1993, 62, 1676-1678.	3.3	20
248	Molecular Orientation of Self-assembled Monolayer of Octadecanethiol on Platinum Surface Studied by Femtosecond Broad-bandwidth Sum Frequency Generation Spectroscopy. Chemistry Letters, 2005, 34, 950-951.	1.3	20
249	Platinum Layer Formation on a Self-assembled Monolayer by Electrochemical Deposition. Chemistry Letters, 2006, 35, 258-259.	1.3	20
250	Metal-Dependent and Redox-Selective Coordination Behaviors of Metalloligand [Mo ^V (1,2-benzenedithiolato) ₃] ^{â^'} with Cu ^I /Ag ^I lons. Inorganic Chemistry, 2011, 50, 2859-2869.	4.0	20
251	Material balance in the O ₂ electrode of Li–O ₂ cells with a porous carbon electrode and TEGDME-based electrolytes. RSC Advances, 2020, 10, 42971-42982.	3.6	20
252	Application of scanning tunnelling microscopy to semiconductor/electrolyte interfaces. Faraday Discussions, 1992, 94, 361.	3.2	19

#	Article	IF	CITATIONS
253	In situ observation of anodic dissolution process of n-GaAs in HCl solution by electrochemical atomic force microscope. Journal of Vacuum Science & Technology an Official Journal of the American Vacuum Society B, Microelectronics Processing and Phenomena, 1994, 12, 1543.	1.6	19
254	Atomic structure of bare p-GaAs(100) and electrodeposited Cu on p-GaAs(100) surfaces in H2SO4 solutions: an AFM study. Journal of Electroanalytical Chemistry, 1996, 409, 45-50.	3.8	19
255	Effect of immobilized electron relay on the interfacial photoinduced electron transfer at a layered inorganic–organic composite film on gold. Journal of Electroanalytical Chemistry, 1998, 455, 229-234.	3.8	19
256	In Situ Electrochemical, Electrochemical Quartz Crystal Microbalance, Scanning Tunneling Microscopy, and Surface X-ray Scattering Studies on Ag/AgCl Reaction at the Underpotentially Deposited Ag Bilayer on the Au(111) Electrode Surface. Journal of Physical Chemistry C, 2011, 115, 12471-12482.	3.1	19
257	A butadiyne-linked diruthenium molecular wire self-assembled on a gold electrode surface. Chemical Communications, 2011, 47, 923-925.	4.1	19
258	Selective dehybridization of DNA–Au nanoconjugates using laser irradiation. Physical Chemistry Chemical Physics, 2013, 15, 15995.	2.8	19
259	Water structure at the interfaces between a zwitterionic self-assembled monolayer/liquid water evaluated by sum-frequency generation spectroscopy. Colloids and Surfaces B: Biointerfaces, 2015, 135, 267-273.	5.0	19
260	Spontaneous pseudo-topological silicon quantization for redesigned Si-based Li-ion batteries. Nano Energy, 2019, 56, 875-883.	16.0	19
261	Electrochemical Growth of Very Long (â^¼80 μm) Crystalline Li ₂ O ₂ Nanowires on Single-Layer Graphene Covered Gold and Their Growth Mechanism. Journal of the American Chemical Society, 2020, 142, 19502-19509.	13.7	19
262	Formation and Novel Functions of Self-assembled Monolayers of Thiol Derivatives. Electrochemistry, 1999, 67, 1105-1113.	1.4	19
263	Accumulation layer formation at n-gallium arsenide/electrolyte interface: photoluminescence probe of the kinetic barrier for hydrogen evolution reaction. The Journal of Physical Chemistry, 1986, 90, 6654-6657.	2.9	18
264	Atomic imaging of an InSe singleâ€crystal surface with atomic force microscope. Journal of Applied Physics, 1993, 74, 1675-1678.	2.5	18
265	Synchronization of electrochemical oscillations with external perturbations. Chemical Physics Letters, 1994, 217, 163-166.	2.6	18
266	In situ observations of atomic resolution image and anodic dissolution process of p-GaAs in HCl solution by electrochemical atomic force microscope. Surface Science, 1994, 311, L737-L742.	1.9	18
267	Real time monitoring of electrochemical deposition of tellurium on Au(111) electrode by optical second harmonic generation technique. Surface Science, 1998, 406, 1-8.	1.9	18
268	Heteroepitaxial growth of CdTe on a p-Si(111) substrate by pulsed-light-assisted electrodeposition. Applied Physics Letters, 2002, 80, 2117-2119.	3.3	18
269	Surface Film Formation and Lithium Underpotential Deposition on Au(111) Surfaces in Propylene Carbonate. Journal of the Electrochemical Society, 2003, 150, A532.	2.9	18
270	Optical Recognition of Surface Chirality at Au(hkl) Single Crystalline Surfaces by Second Harmonic Generation Rotational Anisotropy. Journal of the American Chemical Society, 2005, 127, 12743-12746.	13.7	18

#	Article	IF	CITATIONS
271	Electrochemical Layer-by-Layer Deposition of Pseudomorphic Pt Layers on Au(111) Electrode Surface Confirmed by Electrochemical and In Situ Resonance Surface X-ray Scattering Measurements. Journal of Physical Chemistry C, 2012, 116, 26464-26474.	3.1	18
272	Boron nitride nanosheets decorated with Au, Au-Ni, Au-Cu, or Au-Co nanoparticles as efficient electrocatalysts for hydrogen evolution reaction. Journal of Electroanalytical Chemistry, 2019, 848, 113312.	3.8	18
273	Photoelectrochemical processes: The prevention of competitive anodic dissolution of the photon absorber in hydrogen production. Energy, 1976, 1, 95-96.	8.8	17
274	Theoretical treatment of the photoelectrochemical production of hydrogen. International Journal of Hydrogen Energy, 1977, 2, 123-138.	7.1	17
275	Photocathodic reactions at p-InP. Solar Energy Materials and Solar Cells, 1983, 7, 421-429.	0.4	17
276	Preparation and characterization of wet poly(vinyl chloride)-polypyrolle composite film. Journal of Polymer Science Part A, 1990, 28, 399-409.	2.3	17
277	In situx-ray standing-wave analysis of electrodeposited Cu monolayers on GaAs(001). Physical Review B, 1998, 58, 10800-10805.	3.2	17
278	Photoswitching of electron transfer property of diarylethene–viologen linked molecular layer constructed on a hydrogen-terminated Si(111) Surface. Thin Solid Films, 2009, 518, 591-595.	1.8	17
279	In situ real-time monitoring of geometric, electronic, and molecular structures at solid/liquid interfaces. Japanese Journal of Applied Physics, 2015, 54, 030102.	1.5	17
280	Ligand effect of SnO ₂ on a Pt–Ru catalyst and the relationship between bond strength and CO tolerance. Catalysis Science and Technology, 2016, 6, 3214-3219.	4.1	17
281	The electrochemistry of cytochrome c. Investigation of the mechanism of the 4,4′-bipyridyl surface modified gold electrode. Journal of Electroanalytical Chemistry and Interfacial Electrochemistry, 1980, 116, 527-537.	0.1	16
282	Effect of platinization on the electrochemical behavior of titanium dioxide electrode in aqueous solutions. The Journal of Physical Chemistry, 1985, 89, 4042-4046.	2.9	16
283	STM characteristics of n-GaAs and p-GaP in electrolyte solution. Journal of Electroanalytical Chemistry and Interfacial Electrochemistry, 1990, 283, 425-433.	0.1	16
284	In-situ STM imaging of n-GaAs during anodic photocorrosion. Journal of Electroanalytical Chemistry and Interfacial Electrochemistry, 1991, 313, 121-128.	0.1	16
285	Title is missing!. Angewandte Chemie, 2003, 115, 3018-3021.	2.0	16
286	Construction of Organic Monolayers with Electron Transfer Function on a Hydrogen Terminated Si(111) Surface via Silicon–Carbon Bond and Their Electrochemical Characteristics in Dark and Under Illumination. Chemistry Letters, 2004, 33, 788-789.	1.3	16
287	Size-Dependent Carrier Dynamics in CdS Nanoparticles by Femtosecond Visible-Pump/IR-Probe Measurements. Journal of Physical Chemistry B, 2006, 110, 14192-14197.	2.6	16
288	Resonant hyper-Raman scattering from carbon nanotubes. Chemical Physics Letters, 2007, 438, 109-112.	2.6	16

#	Article	IF	CITATIONS
289	Electrochemical, photoelectrochemical, electrocatalytic and catalytic reduction of redox proteins. Nature, 1980, 285, 673-674.	27.8	15
290	Photoelectrochemical Generation of Hydrogen at Electrochemically Deposited p â€â€‰CdTe Films: Effect of Heatâ€Treatment, Surface Modification by Platinum and Surface Oxide Layer on Conversion Efficiency. Journal of the Electrochemical Society, 1986, 133, 266-271.	2.9	15
291	Laser spot scanning in photoelectrochemical systems, relation between spot size and spatial resolution of the photocurrent. Journal of Applied Physics, 1991, 69, 2324-2327.	2.5	15
292	Coupling of Ground-State Molecular Vibrations to Low-Energy Electronic Transition of Ruthenium(III,II) Porphyrin Dimers. Journal of the American Chemical Society, 2000, 122, 9032-9033.	13.7	15
293	Second harmonic generation study on electrochemical deposition of palladium on a polycrystalline gold electrode. Journal of Electroanalytical Chemistry, 2002, 524-525, 184-193.	3.8	15
294	Photophysical and photoelectrochemical characteristics of multilayers of CdS nanoclusters. Faraday Discussions, 2004, 125, 39.	3.2	15
295	Immobilization of a Binuclear Ruthenium(III) Complex on a Gold (111) Surface: Observations of Proton-coupled Electron Transfer and Electrochemical Durability in Aqueous Media. Chemistry Letters, 2006, 35, 1178-1179.	1.3	15
296	Construction of self-assembled monolayer terminated with N-heterocyclic carbene–rhodium(I) complex moiety. Surface Science, 2007, 601, 5127-5132.	1.9	15
297	Probing the Molecular Conformation of Self-Assembled Monolayers at Metal/Semiconductor Interfaces by Vibrational Sum Frequency Generation Spectroscopy. Journal of Physical Chemistry C, 2009, 113, 21139-21146.	3.1	15
298	Improved charging performance of Li–O2 batteries by forming Ba-incorporated Li2O2 as the discharge product. Journal of Power Sources, 2017, 353, 138-143.	7.8	15
299	Heterocyclic Ringâ€Opening of Nanographene on Au(111). Angewandte Chemie - International Edition, 2021, 60, 9427-9432.	13.8	15
300	Formation of Molecularly Ordered Domain of 1-Decanethiol in the Mixed Self-Assembled Monolayer with Bis(4-pyridyl)disulfide - A Scanning Tunneling Microscopy Observation. Chemistry Letters, 1997, 26, 987-988.	1.3	14
301	Tip-induced nanoscale electrochemical deposition of palladium and platinum on an Au(111) electrode surface. Applied Physics A: Materials Science and Processing, 1998, 66, S457-S461.	2.3	14
302	Scanning tunnelling microscopy study of the self assembly of 2-mercaptopyrimidine and 4,6-dimethyl-2-mercaptopyrimidine on Au(111). Journal of the Chemical Society, Faraday Transactions, 1998, 94, 1315-1319.	1.7	14
303	In Situ Observation of the Two-Dimensional Crystals of Alkanes on a Reconstructed Au(100) Surface in Neat Liquid by Scanning Tunneling Microscopy. Langmuir, 2000, 16, 4413-4415.	3.5	14
304	Probing a molecular electronic transition by two-colour sum-frequency generation spectroscopy. Applied Surface Science, 2003, 212-213, 797-803.	6.1	14
305	Effects of Electrolytes on the Redox Potential and the Rate of the CO Dissociation Reaction of Trinuclear Ruthenium Monocarbonyl Complexes Self-Assembled on an Au(111) Electrode Surface. Bulletin of the Chemical Society of Japan, 2007, 80, 1368-1376.	3.2	14
306	Spontaneous Rapid Growth of Triruthenium Cluster Multilayers on Gold Surface. Cyclic Voltammetric In Situ Monitoring and AFM Characterization. Chemistry Letters, 2008, 37, 576-577.	1.3	14

#	Article	IF	CITATIONS
307	Electrochemical quartz crystal microbalance study on the oxygen reduction reaction in Li+ containing DMSO solution. Journal of Electroanalytical Chemistry, 2014, 716, 49-52.	3.8	14
308	Oxygen Reduction Reaction Catalyzed by Small Gold Cluster on h-BN/Au(111) Support. Electrocatalysis, 2018, 9, 182-188.	3.0	14
309	Pt Nano-Layer Formation by Redox Replacement of Cu Adlayer on Au(111) Surface. Bulletin of the Korean Chemical Society, 2009, 30, 2875-2876.	1.9	14
310	Electroluminescence at pâ€ŧype semiconductor/electrolyte interfaces. Zeitschrift Fur Elektrotechnik Und Elektrochemie, 1987, 91, 447-450.	0.9	13
311	Fiber optical laser spot microscope: A new concept for photoelectrochemical characterization of semiconductor electrodes. Applied Physics Letters, 1988, 53, 965-967.	3.3	13
312	Photoelectrochemical Properties of a GaP Electrode with an n/p Junction. Journal of the Electrochemical Society, 1989, 136, 524-528.	2.9	13
313	Dissipation Structure of Electrochemical Hydrodynamic Convection. The Journal of Physical Chemistry, 1996, 100, 714-717.	2.9	13
314	Mass transport accompanied with electron transfer between the gold electrode modified with 11-ferrocenylundecanethiol monolayer and redox species in solution — an electrochemical quartz crystal microbalance study. Journal of Electroanalytical Chemistry, 1997, 434, 115-119.	3.8	13
315	Effect of Excitation Wavelength on Ultrafast Electron–Hole Recombination in Titanium(IV) Oxide Powders Irradiated by Femtosecond Laser Pulses. Chemistry Letters, 2005, 34, 694-695.	1.3	13
316	Formation of continuous platinum layer on top of an organic monolayer by electrochemical deposition followed by electroless deposition. Journal of Electroanalytical Chemistry, 2011, 662, 80-86.	3.8	13
317	Synthesis and Properties of the Cyano Complex of Oxo-Centered Triruthenium Core [Ru ₃ (μ ₃ -O)(μ-CH ₃ COO) ₆ (pyridine) ₂ (CN)]. Inorganic Chemistry, 2014, 53, 1288-1294.	4.0	13
318	Nitrogen-doped carbon materials derived from acetonitrile and Mg-Co-Al layered double hydroxides as electrocatalysts for oxygen reduction reaction. Electrochimica Acta, 2016, 212, 47-58.	5.2	13
319	Various Active Metal Species Incorporated within Molecular Layers on Si(111) Electrodes for Hydrogen Evolution and CO ₂ Reduction Reactions. Journal of Physical Chemistry C, 2016, 120, 16200-16210.	3.1	13
320	Electrical Matching at Metal/Molecule Contacts for Efficient Heterogeneous Charge Transfer. ACS Nano, 2018, 12, 1228-1235.	14.6	13
321	Electrochemical Atomic Force Microscopy Study on the Surface Structure of a Lead Electrode during Redox Processes and Surface Atomic Arrangement of Electrochemically Formed PbSO4in H2SO4Solution. Langmuir, 1997, 13, 3557-3562.	3.5	12
322	Formation Process and Solvent-Dependent Structure of a Polyproline Self-Assembled Monolayer on a Gold Surface. Langmuir, 2011, 27, 11951-11957.	3.5	12
323	Charge transport at the interface of n-GaAs (100) with an aqueous HCl solution: Electrochemical impedance spectroscopy study. Semiconductors, 2012, 46, 471-477.	0.5	12
324	Effect of surface treatment with different sulfide solutions on the ultrafast dynamics of photogenerated carriers in GaAs(100). Applied Surface Science, 2013, 267, 185-188.	6.1	12

#	Article	IF	CITATIONS
325	Sum-frequency generation analyses of the structure of water at amphoteric SAM–liquid water interfaces. Colloids and Surfaces B: Biointerfaces, 2014, 121, 264-269.	5.0	12
326	Enhanced energy capacity of lithium-oxygen batteries with ionic liquid electrolytes by addition of ammonium ions. Journal of Power Sources, 2017, 356, 12-17.	7.8	12
327	Electrochemical and Electrogenerated Chemiluminescence Properties of a Tris (bipyridyl) ruthenium(II)-Alkanethiol Derivative on ITO and Gold Electrodes. Electrochemistry, 1993, 61, 816-817.	0.3	12
328	Photoproduction of hydrogen: Potential dependence of the quantum efficiency as a function of wavelength. Energy, 1976, 1, 143-145.	8.8	11
329	Photoelectrochemical and Photoluminescence (PL) Properties of p-Type Porous Silicon/Electrolyte Solution Interface:Â Potential Dependent PL Spectra as a Result of Size Dependent Quenching. Journal of Physical Chemistry B, 1997, 101, 4978-4981.	2.6	11
330	Self-Assembled Monolayers of Non-Heme Diiron(III) Model Complexes on Au(111) Electrode: Synthesis and Proton-Coupled Redox Behavior in Water. Chemistry Letters, 1999, 28, 1097-1098.	1.3	11
331	Multicomponent Molecular Layers that Exhibit Electrochemical Potential Flip on Au(111) by Use of Proton-coupled Electron-transfer Reactions. Chemistry Letters, 2008, 37, 684-685.	1.3	11
332	In Situ Scanning Tunneling Microscopy Observation of Metal–Cluster Redox Interconversion and CO Dissociation Reactions at a Solution/Au(111) Interface. Bulletin of the Chemical Society of Japan, 2009, 82, 1227-1231.	3.2	11
333	Photoelectrochemical Reduction of Carbon Dioxide at Si(111) Electrode Modified by Viologen Molecular Layer with Metal Complex. Chemistry Letters, 2012, 41, 328-330.	1.3	11
334	Size dependent lattice constant change of thiol self-assembled monolayer modified Au nanoclusters studied by grazing incidence x-ray diffraction. Electrochemistry Communications, 2016, 65, 35-38.	4.7	11
335	Kinetic Behavior of Catalytic Active Sites Connected with a Conducting Surface through Various Electronic Coupling. Journal of Physical Chemistry C, 2016, 120, 2159-2165.	3.1	11
336	Effect of Water and HF on the Distribution of Discharge Products at Li–O ₂ Battery Cathode. ACS Applied Energy Materials, 2018, 1, 3434-3442.	5.1	11
337	Quantitative cross-sectional mapping of nanomechanical properties of composite films for lithium ion batteries using bimodal mode atomic force microscopy. Journal of Power Sources, 2019, 413, 29-33.	7.8	11
338	EFFECT OF THE Ru+++TREATMENT ON THE ELECTROCHEMICAL HYDROGEN EVOLUTION REACTION AT GaAs ELECTRODES. Chemistry Letters, 1984, 13, 953-956.	1.3	10
339	IR study of the photoanodic oxidation of hexacyanoferrate(4-) at the n-gallium arsenide electrode. The Journal of Physical Chemistry, 1990, 94, 4623-4627.	2.9	10
340	System parameter estimation by evolutionary strategy. , 1996, , .		10
341	In situ observation of anodic dissolution process of p-GaAs(001) in HCl solution by surface X-ray diffraction. Journal of Electroanalytical Chemistry, 1997, 429, 13-17.	3.8	10
342	Visible Electroluminescence from nâ€Type Porous Silicon/Electrolyte Solution Interfaces: Timeâ€Dependent Electroluminescence Spectra. Journal of the Electrochemical Society, 1999, 146, 4166-4171.	2.9	10

#	Article	IF	CITATIONS
343	Formation and Electrochemical Characteristics of Multilayers of Au Nanoclusters Covered by Mixed Self-Assembled Monolayers of Three Kinds of Alkanethiols with Methyl, Ferrocene, or Carboxylate Terminal Group on Au(111) Surface. Chemistry Letters, 2001, 30, 930-931.	1.3	10
344	Structure identification in Takagi-Sugeno fuzzy modeling. , 0, , .		10
345	Eggplant classification using artificial neural network. , 0, , .		10
346	Evolution strategies based particle filters for state and parameter estimation on nonlinear models. , 0, , .		10
347	Luminescent properties of CdS nanoclusters dispersed in solution—Effects of size and surface termination. Journal of Photochemistry and Photobiology A: Chemistry, 2006, 178, 156-161.	3.9	10
348	Sequential layer-by-layer growth of Au nanoclusters protected by a mixed self-assembled monolayer with a polymer binding layer – Effects of pH and ionic strength of the polymer solution. Journal of Electroanalytical Chemistry, 2008, 612, 105-111.	3.8	10
349	Effect of Coating by Perfluorosulfonated Ionomer Film on Electrochemical Behaviors of Pt(111) Electrode in Acidic Solutions. Chemistry Letters, 2010, 39, 286-287.	1.3	10
350	Orientation dependence of Pd growth on Au electrode surfaces. Journal of Physics Condensed Matter, 2010, 22, 474002.	1.8	10
351	Origin of the enhancement of electrocatalytic activity and durability of PtRu alloy prepared from a hetero bi-nuclear Pt–Ru complex for methanol oxidation reactions. RSC Advances, 2013, 3, 15094.	3.6	10
352	Fast Structure Determination of Electrode Surfaces for Investigating Electrochemical Dynamics Using Wavelength-Dispersive X-ray Crystal Truncation Rod Measurements. Journal of Physical Chemistry C, 2017, 121, 24726-24732.	3.1	10
353	Electrochemical SERS observation of molecular adsorbates on Ru/Pt-modified Au(111) surfaces using sphere-plane type gap-mode plasmon excitation. Journal of Electroanalytical Chemistry, 2017, 800, 151-155.	3.8	10
354	Atomistic Control of Metal–Molecule Junctions for Efficient Photo-Induced Uphill Charge Transfer. Journal of Physical Chemistry C, 2020, 124, 18173-18180.	3.1	10
355	Electrochemical and Infrared Spectroelectrochemical Characterization of Self-Assembled Monolayers of a Carbonyl-Coordinated Trinuclear Ruthenium Complex on a Gold Electrode. Electrochemistry, 1999, 67, 1162-1164.	1.4	10
356	The Apparent Molar Volumes of Tetraalkylammonium Halides in Liquid Sulfur Dioxide. Bulletin of the Chemical Society of Japan, 1972, 45, 871-874.	3.2	9
357	Photoelectrochemical Characteristics of Semiconductorâ€Metal/SPE/Metal Cells. Journal of the Electrochemical Society, 1983, 130, 2179-2184.	2.9	9
358	Evidence for inversion layer formation at the p-type gallium arsenide/persulfate solution interface under strong cathodic bias: electroluminescence caused by carrier injection. The Journal of Physical Chemistry, 1984, 88, 4197-4199.	2.9	9
359	Electrochemical Behavior of p-Type Indium Selenide Single Crystal Electrodes in Dark and under Illumination. Bulletin of the Chemical Society of Japan, 1986, 59, 599-605.	3.2	9
360	Structural study of self-assembled monolayers of ferrocenylalkanethiols on gold by angleresolved X-ray photoelectron spectroscopy. Applied Organometallic Chemistry, 1992, 6, 533-536.	3.5	9

#	Article	IF	CITATIONS
361	A Photoelectrochemical Fixation of Carbon Dioxide. Spontaneous Up Quality Conversion of Organic Compound. Chemistry Letters, 1993, 22, 1747-1750.	1.3	9
362	Adaptive identification of non-stationary systems with multiple forgetting factors. , 0, , .		9
363	Conformational Order of Octadecanethiol (ODT) Monolayer at Gold/Solution Interface: Internal Reflection Sum Frequency Generation (SFG) Study. Studies in Surface Science and Catalysis, 2001, , 705-710.	1.5	9
364	Block oriented nonlinear model identification by evolutionary computation approach. , 0, , .		9
365	Formation and electric property measurement of nanosized patterns of tantalum oxide by current sensing atomic force microscope. Journal of Applied Physics, 2003, 94, 7733.	2.5	9
366	Electrodeposition of Flattened Cu Nanoclusters on a p-GaAs(001) Electrode Monitored by in situ Optical Second Harmonic Generation. Journal of Physical Chemistry B, 2005, 109, 5021-5032.	2.6	9
367	Photoanodic formation of an organic monolayer on a hydrogen-terminated Si(111) surface via Si–C covalent bond using a Grignard reagent and its application for one-step monolayer-patterning. Journal of Electroanalytical Chemistry, 2007, 599, 344-348.	3.8	9
368	Electrochemical oxidative formation of ordered monolayers of thiol molecules on Au(111) surface. Chemical Record, 2009, 9, 199-209.	5.8	9
369	Construction of multilayers of bare and Pd modified gold nanoclusters and their electrocatalytic properties for oxygen reduction. Science and Technology of Advanced Materials, 2011, 12, 044606.	6.1	9
370	Humidity dependent structure of water at the interfaces between perfluorosulfonated ionomer thin film and Pt and HOPG studied by sum frequency generation spectroscopy. Electrochemistry Communications, 2013, 27, 5-8.	4.7	9
371	Electrochemical and infrared spectroscopic study of the self-assembled monolayer of a cyano-bridged dimeric triruthenium complex on gold surface. Journal of Electroanalytical Chemistry, 2014, 714-715, 51-55.	3.8	9
372	In situ determination of electronic structure at solid/liquid interfaces. Journal of Electron Spectroscopy and Related Phenomena, 2017, 221, 88-98.	1.7	9
373	1,n-Alkanedithiol (n = 2, 4, 6, 8, 10) Self-Assembled Monolayers on Au(111): Electrochemical and Theoretical Approach. Bulletin of the Korean Chemical Society, 2009, 30, 2549-2554.	1.9	9
374	Characterization of semiconductors by photoluminescence and electroluminescence measurements in electrolyte solutions. TrAC - Trends in Analytical Chemistry, 1990, 9, 98-103.	11.4	8
375	Photon emission via surface state at the gold/acetonitrile solution interface. The Journal of Physical Chemistry, 1991, 95, 779-783.	2.9	8
376	Real time scanning tunneling microscope imaging of Sn electrodeposition on n-GaAs. Journal of Electroanalytical Chemistry, 1992, 337, 217-227.	3.8	8
377	Visible Electroluminescence from p-Type Porous Silicon in Electrolyte Solution. The Journal of Physical Chemistry, 1996, 100, 4564-4570.	2.9	8
378	Multi-objective structure selection for radial basis function networks based on genetic algorithm. , 0, , .		8

#	Article	IF	CITATIONS
379	Evolution Strategies Based Gaussian Sum Particle Filter for Nonlinear State Estimation. , 0, , .		8
380	Partial stripping of Ag atoms from silver bilayer on a Au(111) surface accompanied with the reductive desorption of hexanethiol SAM. Journal of Solid State Electrochemistry, 2009, 13, 1141-1145.	2.5	8
381	Monolayer Formation of a Pt–Ru Dinuclear Complex on a Gold (111) Surface and Its Conversion to a Pt–Ru Two-dimensional Nanocomposite Having Electrocatalytic Activity. Chemistry Letters, 2009, 38, 148-149.	1.3	8
382	Direct proof of potential dependent oxygen adsorption on a gold electrode surface by electrochemical quartz crystal microbalance. Electrochemistry Communications, 2013, 34, 33-36.	4.7	8
383	Broader energy distribution of CO adsorbed at polycrystalline Pt electrode in comparison with that at Pt(111) electrode in H2SO4 solution confirmed by potential dependent IR/visible double resonance sum frequency generation spectroscopy. Electrochimica Acta, 2017, 235, 280-286.	5.2	8
384	Application of windowless energy dispersive spectroscopy to determine Li distribution in Li-Si alloys. Applied Physics Letters, 2018, 112, .	3.3	8
385	Lithiation Products of a Silicon Anode Based on Soft X-ray Emission Spectroscopy: A Theoretical Study. Journal of Physical Chemistry C, 2018, 122, 11096-11108.	3.1	8
386	Investigation of the effects of Pt/Pd composition and PVP content on the activity of Pt/Pd core-shell catalysts. Electrochemistry Communications, 2020, 115, 106736.	4.7	8
387	Preparation of Tantalum Anodic Oxide Film in Citric Acid Solution - Evidence and Effects of Citrate Anion Incorporation. Journal of Electrochemical Science and Technology, 2013, 4, 163-170.	2.2	8
388	In Situ, Real Time Monitoring of Electrode Surfaces by STM II. Surface Structure of n-GaAs During Photoanodic Dissolution. Electrochemistry, 1989, 57, 1213-1214.	0.3	8
389	Photopotential Behavior of Platinized TiO2 Particles. Journal of the Electrochemical Society, 1982, 129, 1752-1753.	2.9	7
390	SYNERGETIC ELECTROCATALYST FOR EFFICIENT PHOTOELECTROCHEMICAL GENERATION OF HYDROGEN AT p-InP. Chemistry Letters, 1984, 13, 301-304.	1.3	7
391	Photon emission at the metal/acetonitrile solution interface: effects of redox species and electrode metal. The Journal of Physical Chemistry, 1992, 96, 4593-4598.	2.9	7
392	Study of the Electronic Structure of GaAs(100) Single Crystal Electrode/Electrolyte Interfaces by Electrochemical Tunneling Spectroscopy. Bulletin of the Chemical Society of Japan, 1996, 69, 275-288.	3.2	7
393	In situOptical Second Harmonic Generation Study of Electrochemical Oxidation of Formaldehyde on a Polycrystalline Platinum Electrode. Chemistry Letters, 1996, 25, 529-530.	1.3	7
394	Evolutionary computation approach to Wiener model identification. , 0, , .		7
395	Evidence for the Diffusion of Au Atoms into the Te UPD Layer Formed on a Au(111) Substrate. Journal of the Electrochemical Society, 2002, 149, C83.	2.9	7
396	Direct Proof for Electrochemical Substitution of Surface Hydrogen of Boron-doped Diamond Electrode by TOF–ESD Method. Chemistry Letters, 2003, 32, 1050-1051.	1.3	7

#	Article	IF	CITATIONS
397	Novel Method for Construction of a Metal–Organic Monolayer–Si Structure Utilizing Thiol-terminated Monolayer Covalently Bonded to the Surface through Si–C Bonds. Chemistry Letters, 2010, 39, 768-770.	1.3	7
398	Construction of a metal–organic monolayer–semiconductor junction on a hydrogen-terminated Si(111) surface via Si–C covalent linkage and its electrical properties. Physical Chemistry Chemical Physics, 2014, 16, 9960.	2.8	7
399	Biofunctionality of Calmodulin Immobilized on Gold Surface Studied by Surface-Enhanced Infrared Absorption Spectroscopy: Ca ²⁺ -Induced Conformational Change and Binding to a Target Peptide. Journal of Physical Chemistry C, 2016, 120, 16035-16041.	3.1	7
400	Electronic Structure of CO Adsorbed on Electrodeposited Pt Thin Layers on Polycrystalline Au Electrodes Probed by Potential-Dependent IR/Visible Double-Resonance Sum Frequency Generation Spectroscopy. Journal of Physical Chemistry C, 2018, 122, 8191-8201.	3.1	7
401	Effects of HF on the Lithiation Behavior of the Silicon Anode in LiPF ₆ Organic Electrolyte Solution. ACS Omega, 2020, 5, 2081-2087.	3.5	7
402	Comment on "Effects of the Helmholtz Layer Capacitance on the Potential Distribution at Semiconductor/Electrolyte Interface and the Linearity of the Mottâ€Schottky Plot―[J. Electrochem. Soc., 130, 895]. Journal of the Electrochemical Society, 1984, 131, 2452-2453.	2.9	6
403	Coverage Dependent Structure of Electrochemically Deposited Cu onp-GaAs(100) in H2SO4Solution Determined byIn SituSurface X-Ray Absorption Fine Structure Spectra. Chemistry Letters, 1997, 26, 761-762.	1.3	6
404	Photopatterning of an Organic Monolayer Formed on a Si Single Crystal Surface via Si–C Covalent Bond by UV Irradiation in an Inert Atmosphere. Japanese Journal of Applied Physics, 2006, 45, 8961-8966.	1.5	6
405	Electrodeposition of Ag and Pd on a reconstructed Au(1 1 1) electrode surface studied by in situ scanning tunneling microscopy. Electrochimica Acta, 2009, 54, 5137-5141.	5.2	6
406	Optical Antenna for Photofunctional Molecular Systems. Chemistry - A European Journal, 2012, 18, 1564-1570.	3.3	6
407	Nanostructuring of Molecular Assembly Using Electrochemical Reductive Desorption of Locally Stabilized Thiol Monolayers. Journal of Physical Chemistry C, 2016, 120, 15823-15829.	3.1	6
408	Electrochemical and in situ SERS study of the role of an inhibiting additive in selective electrodeposition of copper in sulfuric acid. Electrochemistry Communications, 2019, 98, 19-22.	4.7	6
409	Electrochemical Epitaxial Growth, Structure, and Electrocatalytic Properties of Noble Metal Thin Films on Au(111) and Au(100). , 2002, , 17-35.		6
410	Formation and Electrochemical Characteristics of Self-Assembled Monolayer of 11-Ferrocenylundecanethiol on Indium-Tin-Oxide. Electrochemistry, 1994, 62, 1269-1275.	0.3	6
411	Electroluminescent Properties ofn-GaAs in Peroxodisulfate Solutions. Transient Behavior and Carrier Concentration Effect on Emission Spectra. Bulletin of the Chemical Society of Japan, 1984, 57, 3247-3252.	3.2	5
412	Backward SPRT Failure Detection System for Detection of Innovation Variance Change. IFAC Postprint Volumes IPPV / International Federation of Automatic Control, 1988, 21, 1153-1157.	0.4	5
413	Surface morphology and reactivity of the Pt-SPE electrode. Journal of Electroanalytical Chemistry and Interfacial Electrochemistry, 1989, 273, 275-281.	0.1	5
414	Adaptive Identification for Abruptly Changing Systems. IFAC Postprint Volumes IPPV / International Federation of Automatic Control, 1991, 24, 1109-1113.	0.4	5

#	Article	IF	CITATIONS
415	Photon emission at metal/solution interface induced by electron injection from solvated electrons. Journal of Vacuum Science and Technology A: Vacuum, Surfaces and Films, 1992, 10, 2981-2984.	2.1	5
416	Photoelectrochemical synthesis of phthalocyanine. Journal of the Chemical Society Perkin Transactions II, 1992, , 1331.	0.9	5
417	Electrochemical measurements under micro-gravity conditions; Diffusion limited reaction observed by potential step experiment. Journal of Electroanalytical Chemistry, 1993, 358, 333-336.	3.8	5
418	Long-Life Excited States of CdS Photocatalytic Particles. Bulletin of the Chemical Society of Japan, 1995, 68, 3049-3053.	3.2	5
419	Structural study of electrochemically deposited copper on p-GaAs(001) by atomic force microscopy and surface X-ray absorption fine structure measurement. Applied Surface Science, 1997, 121-122, 102-106.	6.1	5
420	Kinetic Coupling of Formaldehyde Oxidation and Oxide Formation on a Platinum Electrode. Bulletin of the Chemical Society of Japan, 1998, 71, 67-71.	3.2	5
421	Cocrystals of 2-AMINO-5-Nitropyridine with Benzenesulfonic Acids for Second-Order Nonlinear Optical Materials. Molecular Crystals and Liquid Crystals, 2004, 420, 79-89.	0.9	5
422	Cyclic Diaminocarbene–Rhodium(I) Complex Tethered to Disulfide: Synthesis and Application to Gold Surface Modification. Chemistry Letters, 2006, 35, 870-871.	1.3	5
423	Drastic Effects on Fibril Formation of Amyloid-β Peptides by the Addition of Amino Acid Residue Units to the Termini. Protein and Peptide Letters, 2010, 17, 458-463.	0.9	5
424	Significant contribution of three-phase boundary for the oxygen reduction current in DMSO solution at a gold disk electrode in hanging meniscus configuration. Journal of Electroanalytical Chemistry, 2013, 707, 151-155.	3.8	5
425	Surface optimization of optical antennas for plasmonic enhancement of photoelectrochemical reactions. Electrochimica Acta, 2013, 112, 864-868.	5.2	5
426	Spectroelectrochemical evidence of the role of viologen moiety as an electron transfer mediator from ITO substrate to a Pt complex acting as a confined molecular catalyst for hydrogen evolution reaction. Electrochemistry Communications, 2016, 62, 56-59.	4.7	5
427	Pt Monolayer Creation on a Au Surface via an Underpotentially Deposited Cu Route. Journal of Physical Chemistry C, 2019, 123, 2872-2881.	3.1	5
428	Computationally empowered design of emerging earth-abundant electrocatalysts towardÂelectron- /proton-transferring energy conversion. Current Opinion in Electrochemistry, 2021, 26, 100661.	4.8	5
429	Reaction Rates in Binary Mixed Solvents. VI. An Sn Ar Reaction in a Methanol-Acetonitrile Mixture. Bulletin of the Chemical Society of Japan, 1971, 44, 2548-2550.	3.2	4
430	Theoretical Aspects of Semiconductor Electrochemistry. Reviews of Physiology, Biochemistry and Pharmacology, 1986, , 1-60.	1.6	4
431	Optimal Input Design for Discrimination of Linear Stochastic Models Based on Kullback–Leibler Discrimination Information Measure. IFAC Postprint Volumes IPPV / International Federation of Automatic Control, 1988, 21, 571-575.	0.4	4
432	Estimation of the relaxation energy of solvated electrons in hexamethylphosphoric triamide solution from photon emission measurements. Journal of Electroanalytical Chemistry and Interfacial Electrochemistry, 1991, 308, 351-356.	0.1	4

#	Article	IF	CITATIONS
433	Scanning tunneling microscopy-tip current voltammetry studies of n-GaAs — effect of illumination, doping density and potential. Journal of Electroanalytical Chemistry, 1992, 336, 57-71.	3.8	4
434	Observation and mechanism of photon emission at metal-solution interfaces. Physical Review B, 1993, 47, 2278-2288.	3.2	4
435	Multi-electron oxidation of formaldehyde on a platinum electrode. Polymers for Advanced Technologies, 1995, 6, 141-143.	3.2	4
436	STM Investigation of Self-Assembly Process of Decanethiol on Au (111). Electrochemistry, 1997, 65, 440-443.	0.3	4
437	The Effects of Nitrogen and Plasma Power on Electrochemical Properties of Boron-Doped Diamond Electrodes Grown by MPCVD. Journal of the Electrochemical Society, 2002, 149, E1.	2.9	4
438	Layer by Layer Construction of Metal–Organic Molecule Bilayer on a Au(111) Surface. Chemistry Letters, 2010, 39, 110-111.	1.3	4
439	Construction of Pt-Ni nanocomposites from Pt-Ni multinuclear complexes on gold(111) surface and their electrocatalytic activity for methanol oxidation. Journal of Electroanalytical Chemistry, 2016, 781, 41-47.	3.8	4
440	Novel In Situ Techniques. , 2017, , 147-174.		4
441	A quantum chemical study of substituent effects on CN bonds in aryl isocyanide molecules adsorbed on the Pt surface. Physical Chemistry Chemical Physics, 2020, 22, 12200-12208.	2.8	4
442	Effect of O2 adsorption on the termination of Li–O2 batteries discharge. Electrochimica Acta, 2020, 340, 135977.	5.2	4
443	A rotating disk electrode study on catalytic activity of iron(II) phthalocyanine-modified electrodes for oxygen reduction in acidic media. Journal of Solid State Electrochemistry, 2021, 25, 141-147.	2.5	4
444	Probing Molecular Mechanisms during the Oscillatory Adsorption of Propyl Chain Functionalized Organosilane Films with Sum Frequency Generation Spectroscopy. Journal of Physical Chemistry B, 2021, 125, 4383-4392.	2.6	4
445	Facile Synthesis Sandwich-Structured Ge/NrGO Nanocomposite as Anodes for High-Performance Lithium-Ion Batteries. Crystals, 2021, 11, 1582.	2.2	4
446	Inversion layer formation and electroluminescence at p-GaAs/persulfate solution interface. Journal of Luminescence, 1984, 31-32, 972-974.	3.1	3
447	Photoluminescent Properties ofp-GaAs/Electrolyte Interface. Evidence for Bandedge Shift during Photoelectrochemical Hydrogen Evolution Reaction. Chemistry Letters, 1986, 15, 1951-1954.	1.3	3
448	Photoluminescence Proof of the Increase of Surface Recombination Velocity atp-GaAs Electrode by Pt Treatment. Chemistry Letters, 1988, 17, 1815-1818.	1.3	3
449	Electrochemical characteristics of silver treated cadmium selenide single crystal electrodes. Journal of Electroanalytical Chemistry and Interfacial Electrochemistry, 1990, 283, 167-176.	0.1	3
450	Photoelectrochemical reactivity of a sulfide treated p-GaAs electrode. Chemical Physics Letters, 1994, 224, 81-85.	2.6	3

#	Article	IF	CITATIONS
451	Time Dependent Electroluminescence Spectra at n-type Porous Silicon/Electrolyte Solution Interface Induced by Hole Injection. Chemistry Letters, 1995, 24, 667-668.	1.3	3
452	Chapter 3. Electrochemistry (1992–1995). Annual Reports on the Progress of Chemistry Section C, 1995, 92, 23-73.	4.4	3
453	Structure of the GaAs(100) Surface During Electrochemical Reactions Determined by Electrochemical Atomic Force Microscopy. ACS Symposium Series, 1997, , 189-201.	0.5	3
454	In Situ Optical and Electrochemical AFM Monitoring of Cu Electrodeposition Process on Bare and (NH[sub 4])[sub 2]S-Treated p-GaAs(001) Surfaces. Journal of the Electrochemical Society, 2000, 147, 3356.	2.9	3
455	Fluctuations of electric variables in Debye–Hückel electrolyte at a neutral hard wall. Electrochimica Acta, 2001, 46, 3051-3055.	5.2	3
456	Nonlinear system identification based on evolutionary fuzzy modeling. , 0, , .		3
457	Femtosecond Visible Pump Mid-IR Probe Study on the Effects of Surface Treatments on Ultrafast Photogenerated Carrier Dynamics in n-GaAs (100) Crystals. Chemistry Letters, 2004, 33, 604-605.	1.3	3
458	Theoretical analysis of the potential distribution and transportation behavior of the ordered alkyl monolayer–silicon junction. Physical Chemistry Chemical Physics, 2006, 8, 5653-5658.	2.8	3
459	Pattern Classification by Evolutionary RBF Networks Ensemble Based on Multi-objective Optimization. , 2006, , .		3
460	Ultrafast Dynamics of Photogenerated Electrons in CdS Nanocluster Multilayers Assembled on Solid Substrates: Effects of Assembly and Electrode Potential. ChemPhysChem, 2013, 14, 2174-2182.	2.1	3
461	Structure of adsorbed molecular layer on fused quartz surface determined sequentially in sodium stearate solution, dry Ar, pure water, and dry Ar by sum frequency generation spectroscopy. Surface Science, 2013, 607, 92-96.	1.9	3
462	In Situ SXS and XAFS Measurements of Electrochemical Interface. , 2016, , 367-449.		3
463	Soft X-ray Li-K and Si-L2, 3 Emission from Crystalline and Amorphous Lithium Silicides in Lithium-Ion Batteries Anode. Journal of the Electrochemical Society, 2019, 166, A5362-A5368.	2.9	3
464	Electrochemical Lithiation and Delithiation of Si(100) Single-crystal Surface. Chemistry Letters, 2020, 49, 91-94.	1.3	3
465	In situ FT-IR Study of p-Type Porous Silicon during Electroluminescence Process. Electrochemistry, 1994, 62, 540-541.	0.3	3
466	Identifying Substrate-Dependent Chemical Bonding Nature at Molecule/Metal Interfaces Using Vibrational Sum Frequency Generation Spectroscopy and Theoretical Calculations. Journal of Physical Chemistry C, 2022, 126, 11298-11309.	3.1	3
467	Integer programming approach to optimal smoothing of two-state Markov sequences. , 0, , .		2
468	Optimal Input Design for Autoregressive Model Discrimination Based on the Kullback-Leibler Discrimination Information. IFAC Postprint Volumes IPPV / International Federation of Automatic Control, 1987, 20, 375-379.	0.4	2

#	Article	IF	CITATIONS
469	Optimal Input Design for Model Discrimination Based on the Kullback Discrimination Information: Frequency Domain Approach. IFAC Postprint Volumes IPPV / International Federation of Automatic Control, 1990, 23, 191-196.	0.4	2
470	Photocurrent generation via vertical transport of a photogenerated electron through electron relay confined within micropores of an anodic aluminium oxide film. Journal of the Chemical Society Chemical Communications, 1990, , 195.	2.0	2
471	Photoelectrochemical kinetics of a photosynthetic cell. Journal of Electroanalytical Chemistry, 1994, 371, 111-116.	3.8	2
472	Effects of electrode potential on nanostructure of single crystalline semiconductor electrodes. Solar Energy Materials and Solar Cells, 1995, 38, 347-348.	6.2	2
473	Optimal auxiliary input for fault detection of systems with model uncertainty. , 0, , .		2
474	Hammerstein model identification method based on genetic programming. , 0, , .		2
475	Spectroscopic Studies on Electroless Deposition of Copper on a Hydrogen-Terminated Si(111) Surface in Fluoride Solutions [Journal of The Electrochemical Society, 148, C421 (2001)]. Journal of the Electrochemical Society, 2001, 148, L6.	2.9	2
476	Ultrafast dynamics in CdSSe-doped glasses. Journal of Materials Science, 2004, 39, 5857-5859.	3.7	2
477	Design of Pt-CeOxhetero-interface on electrodes in polymer electrolyte membrane fuel cells. IOP Conference Series: Materials Science and Engineering, 2014, 54, 012010.	0.6	2
478	Organic Molecular Layer with High Electrochemical Bistability: Synthesis, Structure, and Properties of a Dynamic Redox System with Lipoate Units for Binding to Au(111). ChemPlusChem, 2017, 82, 1043-1047.	2.8	2
479	Heterocyclic Ringâ€Opening of Nanographene on Au(111). Angewandte Chemie, 2021, 133, 9513-9518.	2.0	2
480	Potential and time dependent broad band sum frequency generation spectroscopic study on electrochemical oxidation of adsorbed CO on Pt(1 1 1) electrode surface in pre-peak region in alkaline solution. Journal of Electroanalytical Chemistry, 2021, 896, 115478.	3.8	2
481	Lithiation of the crystalline silicon as analyzed using soft X-ray emission spectroscopy and windowless energy dispersive X-ray spectroscopy. Applied Surface Science, 2021, 569, 151040.	6.1	2
482	In-situ Electrochemical AFM Study of Semiconductor Electrodes in Electrolyte Solutions. , 0, , 253-265.		2
483	Electrocatalytic Activity for Oxygen Reduction of Multilayer of Pd Coated Gold Nanoclusters. Transactions of the Materials Research Society of Japan, 2008, 33, 1093-1096.	0.2	2
484	Preparation of Tantalum Anodic Oxide Film in Citric Acid Solution - Evidence and Effects of Citrate Anion Incorporation. Journal of Electrochemical Science and Technology, 2013, 4, 163-170.	2.2	2
485	Studies of the "Electrochemistry of Ordered Interfaces―for a Better Society. Electrochemistry, 1999, 67, 1104-1104.	1.4	2
486	Charge Transfer Reaction Inverse Photoemission Spectroscopy (CTRIPS) at a Gold/Acetonitrile Solution Interface. Evidence for Photon Emission via Surface States. Chemistry Letters, 1990, 19, 1159-1162.	1.3	1

#	Article	IF	CITATIONS
487	Electrostatic Kerr effect at a potentiostatically controlled liquidvbliquid interface. Journal of Electroanalytical Chemistry, 1995, 396, 397-399.	3.8	1
488	Optimal smoothing of binary Markov sequences by genetic algorithm and its application to image restoration. , 0, , .		1
489	Hammerstein model identification using genetic programming. , 0, , .		1
490	放射å‰ã«ã,~ã,‹é›»æ°—化å¦ååįœæ€§è©•価. Hyomen Gijutsu/Journal of the Surface Finishing Society (of Jaµ2 an, 2	ООЗ, 54, 968
491	Cocrystals of 2-AMINO-5-Nitropyridine with Benzenesulfonic Acids for Second Order Nonlinear Optical Materials. Molecular Crystals and Liquid Crystals, 2004, 414, 77-86.	0.9	1
492	Pattern Classification by Evolutionary RBF Networks Ensemble Based on Multi-objective Optimization. , 0, , .		1
493	Effect of Electrode Potential on Ag Electrodeposition on a Reconstructed Au(111) Electrode Surface. Hyomen Kagaku, 2008, 29, 621-628.	0.0	1
494	Electrochemical Reduction of Oxygen in Organic Solvents With and Without Li+ Cation – Effect of Oxygen Supply. ECS Meeting Abstracts, 2013, , .	0.0	1
495	Electrochemistry of rechargeable lithium–air batteries. , 2015, , 149-181.		1
496	Structural Study of Electrochemically Lithiated Si. ECS Transactions, 2017, 75, 67-72.	0.5	1
497	Solid–Liquid Interfaces. , 2017, , 505-525.		1
498	Interfacial Molecular Structure and Dynamics at Solid Surface Studied by Sum Frequency Generation Spectroscopy. , 2017, , 203-241.		1
499	Surface X-ray Scattering Technique for Electrode-In situ Structural Study on Electrodeposited Metal Layers on Au(111) Single Crystal Electrode Hyomen Kagaku, 2003, 24, 734-739.	0.0	1
500	Sum Frequency Generation Studies on the Hydrogen Terminated Si Surface. Shinku/Journal of the Vacuum Society of Japan, 2004, 47, 439-445.	0.2	1
501	Investigation of Interfacial Structure of Electrode/Electrolyte Interfaces by Nonlinear Spectroscopic Techniques. Hyomen Kagaku, 2006, 27, 595-600.	0.0	1
502	Nonlinear Raman Scattering Spectroscopy for Carbon Nanomaterials. , 2012, , 99-118.		1
503	Effect of Water on the Product Distribution at the Cathode of Li-O ₂ Batteries. ECS Meeting Abstracts, 2017, MA2017-01, 305-305.	0.0	1
504	Response to "Comment on â€~Effects of the Helmholtz Layer Capacitance on the Potential Distribution at Semiconductor/Electrolyte Interface and the Linearity of the Mottâ€6chottky Plot'―[J. Electrochem. Soc., 130, 895]. Journal of the Electrochemical Society, 1984, 131, 2453-2453.	2.9	0

#	Article	IF	CITATIONS
505	TPD Detection of Hydrogen Absorbed in GaAs during Electrochemical Hydrogen Evolution Reaction. Chemistry Letters, 1987, 16, 2301-2304.	1.3	0
506	Thin films-preparation, structure and properties. Electrochemical deposition and structure of CdSexTe1-x thin films Nippon Kagaku Kaishi / Chemical Society of Japan - Chemistry and Industrial Chemistry Journal, 1987, 1987, 2006-2009.	0.1	0
507	Photoanodic behavior of n-InSe single crystal Nippon Kagaku Kaishi / Chemical Society of Japan - Chemistry and Industrial Chemistry Journal, 1988, 1988, 1157-1162.	0.1	0
508	A hybrid neural network for principal component analysis. , 0, , .		0
509	Adaptive Optimization in Non-Stationary Environments with Hierarchical Learning. IFAC Postprint Volumes IPPV / International Federation of Automatic Control, 1993, 26, 875-880.	0.4	0
510	Comment on photoelectrochemistry. Solar Energy Materials and Solar Cells, 1995, 38, 321-322.	6.2	0
511	Optimal auxiliary input for fault detection and fault diagnosis. , 0, , .		0
512	Evolutionary approach for improvement of the operational route for mobile robots. , 0, , .		0
513	Optimal auxiliary input for fault detection based on Kullback divergence. , 0, , .		0
514	Wiener model identification by evolutionary computation approach with piecewise linearization. , 0, , .		0
515	Operating regime determination in fuzzy local modeling by genetic algorithm. , 0, , .		0
516	In Situ Study of Ultrathin Film Formation on Au(111) Surface in Propylene Carbonate by Scanning Tunneling Microscopy under Potential Control. Journal of the Electrochemical Society, 2002, 149, E286.	2.9	0
517	In Situ Real Time Investigation on the Structure at Electrode/Electrolyte Interfaces by Surface X-Ray Scattering. ECS Meeting Abstracts, 2010, , .	0.0	0
518	Characterization of Structure and Function of Biointerfaces by Surface Vibrational Spectroscopy. Oleoscience, 2011, 11, 197-203.	0.0	0
519	Important Role of Cerium Oxide in Oxygen Reduction Reaction at Pt-CeOx Nanocomposite Electrocatalyst Studied by in situ Electrochemical XAFS. ECS Meeting Abstracts, 2012, , .	0.0	0
520	Application of Resonance Surface X-ray Scattering Technique to Solid/Liquid Interfaces. Hyomen Kagaku, 2013, 34, 385-388.	0.0	0
521	Self-Assembly: Formation of Functionalized Nanowires by Control of Self-Assembly Using Multiple Modified Amyloid Peptides (Adv. Funct. Mater. 39/2013). Advanced Functional Materials, 2013, 23, 4880-4880.	14.9	0
522	Structural Transition of Alkylthiol/Au(111) Interface During Self-Assembly Process. ECS Meeting Abstracts, 2013, , .	0.0	0

#	Article	IF	CITATIONS
523	Adsorption and Desorption Behavior of Nafion on Au and Pt Surfaces. Hyomen Kagaku, 2015, 36, 465-473.	0.0	0
524	<i>In situ</i> Structural Study of Electrode/Electrolyte Interfaces by SXS Using Synchrotron Radiation. Hyomen Kagaku, 2016, 37, 72-77.	0.0	0
525	Editorial overview Electrochemical surface science and energy conversion. Current Opinion in Electrochemistry, 2019, 17, A4-A7.	4.8	Ο
526	Anomalously Slow Conformational Change Dynamics of Polar Groups Anchored to Hydrophobic Surfaces in Aqueous Media. Chemistry - an Asian Journal, 2020, 15, 3321-3325.	3.3	0
527	Title is missing!. Shinku/Journal of the Vacuum Society of Japan, 2004, 47, 529-534.	0.2	Ο
528	Observation of Solid/Solution Interface Structures in Atomic and Molecular Resolution. Hyomen Kagaku, 2006, 27, 576-580.	0.0	0
529	STM Studies on Molecular Assembly at Solid/Liquid Interfaces. Nanoscience and Technology, 2007, , 65-100.	1.5	0
530	Layer-by-Layer Assembly of Gold Nanoclusters with Self-Assembled Monolayers. , 2008, , 1773-1783.		0
531	Expectations and Challenges for Fuel Cell. Hyomen Kagaku, 2011, 32, 681-681.	0.0	Ο
532	Semiconductor Electrode. , 2014, , 1875-1882.		0
533	Novel Approaches for the Study of Surface Structure and Reactivity of Semiconductor Electrodes. , 1992, , 193-203.		Ο
534	Local structures of isovalent and heterovalent dilute impurities in Si crystal probed by fluorescence x-ray absorption fine structure. Nihon Kessho Gakkaishi, 1997, 39, 116-116.	0.0	0
535	Frontiers of Photo-catalysis and Photo-reaction at Solid Surfaces. Visible-Light-Induced Electron Transfer at Electrodes Modified with Self-Assembled Monolayers Hyomen Kagaku, 1999, 20, 108-114.	0.0	Ο
536	Cobalt Phthalocyanine Analogues As Soluble Catalysts That Improve the Charging Performance of Li-O2 Batteries. ECS Meeting Abstracts, 2016, , .	0.0	0
537	The Effects of Water Concentration on Lithium Deposition/Dissolution Toward Practical Operation of Lithium-Air Batteries. ECS Meeting Abstracts, 2016, , .	0.0	Ο
538	Insulating Boron Nitride Nanosheet on Inert Gold Electrode As a Novel Efficient Electrocatalyst for Oxygen Reduction Reaction. ECS Meeting Abstracts, 2016, , .	0.0	0
539	Structural Study of Electrochemically Lithiated Si. ECS Meeting Abstracts, 2016, , .	0.0	0
540	Electrochemical Lithiation/Delithiation Process of Si. ECS Meeting Abstracts, 2016, , .	0.0	0

#	Article	IF	CITATIONS
541	Utilization of Hard X-Ray Photoelectron Spectroscopy for Silicon-Based Negative Electrodes Buried within Solid Electrolyte Interphase. ECS Meeting Abstracts, 2016, , .	0.0	0
542	Insulating Boron Nitride Nanosheet on Inert Gold Substrate As a Novel Electrocatalyst for Oxygen Reduction Reaction - Theoretical and Experimental Investigations. ECS Meeting Abstracts, 2016, , .	0.0	0
543	Potential Dependent IR/Visible Double Resonance Sum Frequency Generation Spectroscopy to Probe Electronic Structure at Electrochemical Interfaces. ECS Meeting Abstracts, 2016, , .	0.0	0
544	High-Speed Surface X-Ray Diffraction for Monitoring Structural Changes of Electrode Surfaces: An Application to Methanol Oxidation on Pt(111). ECS Meeting Abstracts, 2016, , .	0.0	0
545	(Invited) Spectroelectrochemical Evidence of an Electron Transfer through Viologen Moiety from an ITO Electrode to a Molecular Catalyst for Hydrogen Evolution Reaction Confined within a Viologen Monolayer. ECS Meeting Abstracts, 2017, , .	0.0	0
546	Insulating Boron Nitride Nanosheet on Inert Gold Substrate As a Highly Efficient Electrocatalyst for Hydrogen Evolution Reaction. ECS Meeting Abstracts, 2017, , .	0.0	0
547	In Situ Structural Determination of Underpotentially Deposited Pd Monolayer on Au(111) Surface. ECS Meeting Abstracts, 2018, , .	0.0	0
548	(Invited) Combination of Insulating Boron Nitride and Inert Gold Substrate As an Efficient Electrocatalysts for Oxygen Reduction Reaction and Hydrogen Evolution Reaction - Theoretical and Experimental Investigations. ECS Meeting Abstracts, 2018, , .	0.0	0
549	(Invited) Boron Nitride Nanosheets Decorated with Small Gold Nanoparticles (~ 5 nm) of Narrow Size Distribution on Gold Substrate As an Efficient Electrocatalyst for Oxygen Reduction to Water. ECS Meeting Abstracts, 2018, , .	0.0	0
550	(Keynote) Electrochemical Surface Science and Energy Conversion. ECS Meeting Abstracts, 2018, , .	0.0	0
551	Cross Sectional Mapping of Nano-Mechanical Properties of Composite Electrodes for Lithium Ion Batteries Using Bimodal Mode Atomic Force Microscopy. ECS Meeting Abstracts, 2019, , .	0.0	0
552	(Invited) Confined Molecular Electrocatalyst for Electrochemical and Photoelectrochemical Hydrogen Evolution Reaction. ECS Meeting Abstracts, 2019, , .	0.0	0
553	(Keynote) Photoelectrochemistry - Looking Back to the Future. ECS Meeting Abstracts, 2019, , .	0.0	0
554	Confined-Space-Induced Side Reactions in Li-O2 Electrochemistry. ECS Meeting Abstracts, 2020, MA2020-02, 746-746.	0.0	0
555	Breathing of Water during Charge/Discharge Cycling in a Nonaqueous Li/O2 Cell with Tetraglyme-Based Electrolytes. ECS Meeting Abstracts, 2020, MA2020-02, 664-664.	0.0	0
556	Hydrogen Evolution Reaction at Metal Treated n-GaAs Electrodes. Electrochemistry, 1986, 54, 940-943.	0.3	0
557	(Digital Presentation) Mass Spectroscopic Products Analysis during Charging of Li-O ₂ Cell with Tegdme Based Electrolyte. ECS Meeting Abstracts, 2022, MA2022-01, 58-58.	0.0	0
558	Effects of Discharge/Charge Cycles on Inner Structures of Laminated Cells of Lithium Air Batteries By X-Ray CT, SEM/EDS and FIB-SEM/EDS. ECS Meeting Abstracts, 2022, MA2022-01, 117-117.	0.0	0